REPORT DOCUMENTATION PAGE

Form Approved
OMB No. 0704-0188

1 AGENCY USE ONLY (Leave blank)	2 REPORT DATE	3 REPORT TYPE AND DATES COVERED
	January 10, 1994	FINAL -- 5/15/91 to 11/14/93

(2)

4 TITLE AND SUBTITLE
PHYSICAL PROCESSES IN SNOWPACKS DURING RAIN OR MELT EVENTS

5 FUNDING NUMBERS
DAAL03-91-G-0143

6 AUTHOR(S)
H. Conway

7. PERFORMING ORGANIZATION NAME(S) AND ADDRESS(ES)
University of Washington
Grant and Contract Services
22 Administration Building, AD-24
Seattle, WA 98195

8. PERFORMING ORGANIZATION REPORT NUMBER

9. SPONSORING / MONITORING AGENCY NAME(S) AND ADDRESS(ES)
U.S. Army Research Office
P. O. Box 12211
Research Triangle Park, NC 27709-2211

10. SPONSORING / MONITORING AGENCY REPORT NUMBER
ARO 28344.1-GS

11. SUPPLEMENTARY NOTES
The view, opinions and/or findings contained in this report are those of the author(s) and should not be construed as an official Department of the Army position, policy, or decision, unless so designated by other documentation.

12a. DISTRIBUTION / AVAILABILITY STATEMENT
Approved for public release; distribution unlimited

12b. DISTRIBUTION CODE

13. ABSTRACT (Maximum 200 words)

Observations during rain-on-snow indicate three evolutionary regimes of snow behavior; immediate avalanching, delayed avalanching, and a return to stability. Immediate avalanching occurs within minutes of the onset of rain. This is important information for avalanche control technicians; the avalanches release several hours before liquid water has penetrated to the sliding layer. Delayed avalanches release several hours after rain has started. The delay varies depending on the rate of increasing stress associated with additional preciptation, and the time taken for water to penetrate and weaken the snowpack. Avalanche activity is rare after continuation of rain for 15 hours or more. This return to stability occurs after a drainage system has been established. Infiltration is not uniform and water penetrates through localized channels that often occupy less than 50% of the total volume of the snowpack. Runoff starts much sooner than would be predicted if wetting was homogeneous. Insitu measurements of deformation indicate that the strain rate in low density snow often increases without increased normal loading. Forces other than gravity must contribute to the deformation. This important finding is supported by measurements on slopes that show that the usual assumption that snow behaves as a linear, isotropic, viscous material is incorrect. A new theory involving thermodynamically induced strain is suggested.

14. SUBJECT TERMS	15. NUMBER OF PAGES
Snow, Rain-On-Snow, Avalanches, Infiltration, Deformation, Rheology	27
	16. PRICE CODE

17. SECURITY CLASSIFICATION OF REPORT	18. SECURITY CLASSIFICATION OF THIS PAGE	19. SECURITY CLASSIFICATION OF ABSTRACT	20. LIMITATION OF ABSTRACT
UNCLASSIFIED	UNCLASSIFIED	UNCLASSIFIED	UL

TABLE OF CONTENTS

STATEMENT OF PROBLEM STUDIED

Rain-on-snow is common in many of the western United States and these events often produce major avalanching and flooding in the region. Avalanches and floods are disruptive and sometimes cause significant losses, including loss of life. Considerable uncertainty is associated with predicting rain-on-snow disasters. Much of the uncertainty is due to difficulties forecasting precipitation in mountain regions, but the problem is further complicated because it is difficult to characterize simply the mechanical and hydrological response of seasonal snow to rain.

It is well known that introduction of liquid water into snow causes rapid changes in the texture and strength of the snow. These rapid changes are dominated by freezing and melting on crystal boundaries caused by intra and inter granular flow of heat and there is a growing understanding of these grain-scale processes. However, there is still a wide gap in understanding how the macroscale behavior is related to microscale processes. The gap in understanding arises in part because of the heterogeneous structure of real snowpacks which results in a complex pattern of water penetration and leads to non-homogeneous wetting. The mechanical properties are altered by the presence of liquid water and so non-homogeneous wetting results in a complicated pattern of stress and strain in the snowpack.

Our approach to understanding the connection between macroscale and microscale behavior has been to make insitu measurements of snow properties with high spatial and temporal resolution. It is not possible to simulate natural conditions in laboratory tests but in field experiments it is not possible to control the initial and boundary conditions. We have documented the conditions and made measurements during a number of different storm cycles to determine the response of snow under a range of conditions. Although this approach is time consuming, it has yielded a number of results and insights that are not immediately apparent from laboratory experiments.

SUMMARY OF IMPORTANT RESULTS

The research has yielded several important results which have practical applications for flood and avalanche prediction. These have been discussed in detail in publications arising from the research (see publications list and appendixes below). Some of the major findings are discussed briefly below:

I. Timing of avalanche release during rain

The potential for avalanche release increases significantly immediately following the onset of rain. This is an important realization that has consequences for planning avalanche hazard control and is discussed in more detail in appendix I. The timing is surprising because it had previously been thought that the avalanches release only after liquid water penetrates and weakens a sub-surface layer. However that implies a delay between the onset of rain and the time of avalanching but our observations and measurements indicate that avalanches often released several hours before water had penetrated to the siding layer.

Immediate avalanche activity is particularly high when the snow stability prior to rain is already close to critical. The climate of the Western States is favorable for producing this condition. The east side of the mountains is influenced mainly by cool Arctic air, while the west side is dominated by relatively wet, warm marine air from the Pacific Ocean. Snow that has accumulated under Arctic type conditions is relatively unstable and therefore particularly prone to avalanching when a strong westerly system moves into the region and causes rapid warming and rain. This means that it is possible to predict the timing of immediate avalanche activity with reasonable accuracy (within an hour) by forecasting the meteorological conditions in the avalanche starting zones. This can be done by monitoring conditions from a network of weather stations surrounding the starting zones and located in the tracks of approaching storms.

Avalanches do not always release immediately after rain starts but they can be delayed several hours. It is thought that the release of these avalanches is related to liquid water penetrating and weakening the snow and also to the increased stress from the weight of the rain. Accurate prediction of the timing is more problematical because it is difficult to accurately define the evolving distribution of liquid water in layered snowpacks. This is discussed in more detail in appendix II. In our experience the delay varied up to thirteen hours after rain started but longer delays have been observed in situations when the snowpack was deep and had not been previously wetted.

II. A return to stability

Even if rain continues, avalanche activity is usually rare after 15 to 24 hours. The return to stability appears to be related to the evolution of a drainage system. Once drainage is established water is less likely to weaken the snowpack or cause the stress to increase. In fact, the stress may decrease as water drains from the snowpack. In some cases it is possible that water at the ground/snow interface could cause large, full-depth avalanches but we did not observe this phenomenon during the study.

III. Infiltration of water into snow

It has been known for some time that liquid water often penetrates snow through discrete fingers or channels. However relatively few studies have been made in real-time. We developed a new technique to track the progress of liquid water through an undisturbed snowpack in real-time. Wetting was tracked by measuring the evolution of snow temperature using a 2-dimensional array of thermistors. The position of the zero degree isotherm defines the position of the wetting front. Details of the experimental technique and measurements are shown in appendix II.

Measurements show the evolution of wetting is influenced strongly by the snow stratigraphy. Vertical flow tends to be impeded and diverted laterally at ice layers and layers of low permeability. On the other hand, water penetrates to depth relatively rapidly in a more homogeneous snowpack. Characterizing infiltration is made more difficult because the hydraulic conductivity may change significantly as a result of grain-coarsening processes associated with wetting. However other things being equal, water will penetrate homogeneous, coarse-grained snowpacks faster than those that contain multiple stratigraphic horizons.

Measurements indicate that water often penetrates through localized channels that occupy less than 50% of the total volume of the snowpack. We are not certain whether this value is typical, but it is apparent that runoff occurs much sooner than would be expected if wetting was homogeneous. Others have shown that liquid water in wet zones becomes mobile only after the water content has increased sufficiently to form a continuous film through the pore spaces. This critical moisture content is known as the "irreducible" moisture content and is strongly dependent on the size and texture of grains. Our measurements indicate that the irreducible water content (θ_i) is about 6% (by volume) and the moisture content of wet zones (θ_w) is typically 8 to 10% during infiltration.

Calculations of heat transfer indicate the rate in dry snow is slow and occurs primarily by conduction. In contrast, the latent heat released when water freezes on contact with cold snow dominates heat transfer at the wetting front. However the energy needed to warm a maritime snowpack to 0 °C is small, and can be supplied by the phase change of a relatively small mass of liquid water. Most of the influx of rain water is available to wet and then drain out of the snowpack. Infiltration of a maritime snowpack is controlled primarily by the hydraulic rather than thermal conditions.

IV. Timing of runoff during rain-on-snow events

Predicting the time of outflow is of interest for flood prediction and also for predicting the return to stability discussed above. The timing of outflow is determined by the rate of precipitation as well as the hydrological properties of the snowpack. The time of runoff (Δt, the time in hours since the onset of rain) can be written:

$$\Delta t = V_w * \theta_w \, h_s / PI$$

where V_w is the fractional volume of wetted snow at the time of runoff, θ_w is the average moisture content of the wetted snow, h_s is the snow depth (m), and PI is the average rate of rainfall (m hr^{-1}).

Maritime snowpacks are generally 1.5 to 3 m deep, and the rate of rainfall can range from 2 to 5 $x10^{-3}$ m hr^{-1}. Using typical values for V_w and θ_w (discussed above), we expect drainage would commence 12 to 72 hours after rain started. These times are comparable to those observed in the field.

V. Deformation and rheological properties of snow

Pre-failure deformation and stresses within snowpacks are of interest for understanding avalanche release mechanisms. Although high density snow ($\rho > 350$ kg m^{-3}) has been successfully modeled as a viscous material, it is not clear that this description is adequate for low density snow. The density of critical layers that control snow slope stability is usually less than 350 kg m^{-3} and grains within these layers are often intricately shaped with a high surface area to volume ratio. It is difficult to make laboratory measurements on low density snow and instead, we have chosen to make insitu measurements of deformation to investigate the mechanical properties of low density snow.

We developed a new technique to resolve the internal deformation of snowpacks in real-time. On horizontal snowpacks we simply measured the vertical motion of velocity shoes using a voltage divider system. A settlement profile was obtained by measuring the position of shoes that had been placed sequentially at the surface as snow accumulated. A similar technique was used to measure vertical motion on inclined snowpacks, and slope parallel velocity was measured separately. We attached a rotary potentiometer to the vertical shoe and ran a cord downslope to a second velocity shoe. More details of these measurements are outlined in our paper *"Insitu measurements of snow deformation"*.

Figure 1 shows the evolution of compaction at the horizontal site during the winter of 1992-93. Rain-on-snow events are marked by arrows. The initial density of the new snow ranged from 60 to 180 kg m^{-3} and three of the accumulation events were followed by rain. Compaction rates were fastest near the surface, even although the compactive stresses near the surface are small. On a number of occasions the measurements indicate that the strain rate in low density snow increased without increased normal loading. This suggests that the assumption of linear, isotropic, viscous behavior is not adequate for low density snow and some other mechanism must be active. We think that thermodynamic processes acting in response to the complex morphology of the micro-structure must influence the deformation of low density snow. Measurements of deformation on slopes substantiate this idea.

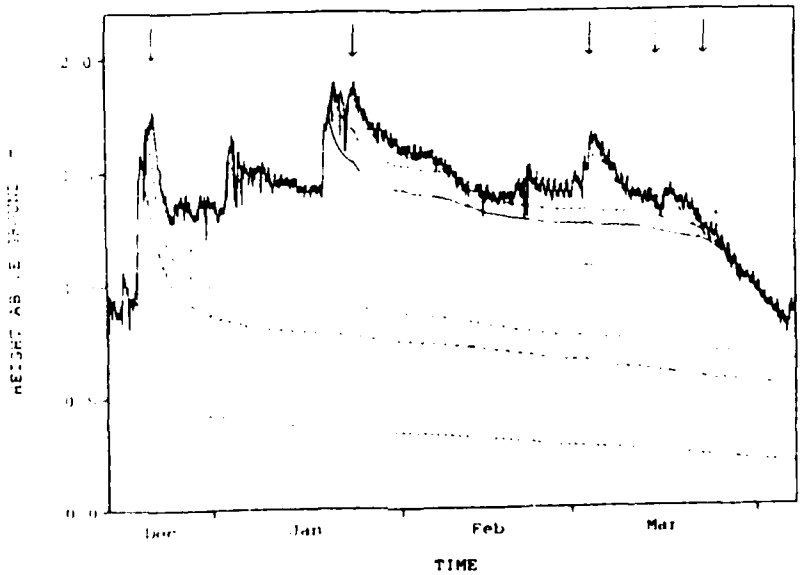

Figure 1. ***Evolution of compaction of a horizontal snowpack during the winter of 1992-93. The initial density of the new snow ranged from 60 to 180 kg m^{-3}. Times of rain-on-snow are marked by arrows.***

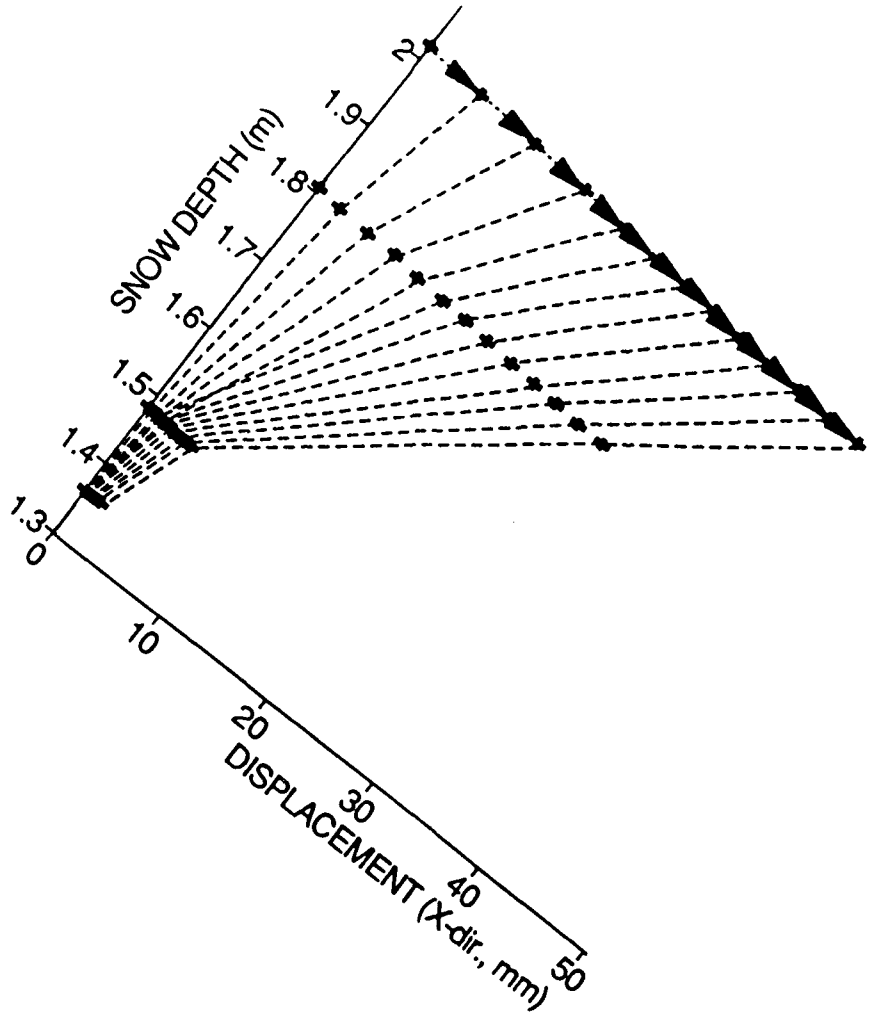

Figure 2. ***Deformation profile of snow on a 36° slope. The material lines are spaced at hourly intervals and start at midday on January 21st, 1993.***

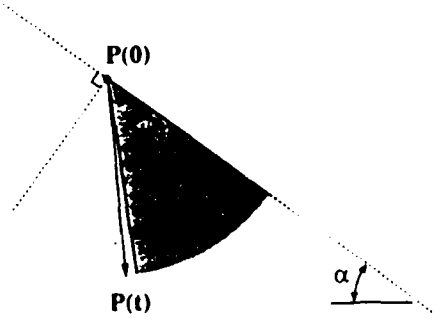

Figure 3. ***Observed and theoretical motion of snow creep on a slope. The shaded area represents the range of motion possible assuming viscoelastic behavior. Observed motion (shown schematically as the motion of particle P) was usually outside this range.***

Figure 2 shows a deformation profile measured in the middle of a 36° slope. The material lines are spaced at hourly intervals starting at midday on January 21st, 1993. Measurements show the creep velocity at the surface (2 to 3 $x10^{-6}$ m s^{-1}) was more than 15x faster than the older snow below. Calculations show the shear strain rate within the upper 200 mm of new snow was about 5 $x10^{-6}$ s^{-1} during the first hour and then it decreased. Laboratory tests by others using samples that were 20 mm thick have shown that failure occurs only if the strain rate exceeds 10^{-4} s^{-1}. We are not certain how to scale these laboratory tests to larger samples. Strain is usually concentrated in relatively thin bands (1 - 2 mm thick) and so a measurement that is averaged over a thicker layer might not represent the maximum value. Our observations and measurements during times of instability indicate that conditions become critical when the shear strain rate approaches 10^{-5} s^{-1} (measured over 200 mm). Following the discussion above, this critical strain rate could easily be equivalent to a rate of 10^{-4} s^{-1} measured over a 20 mm sample, or 10^{-3} s^{-1} measured over a 2 mm shear band. It would be useful to make more measurements with increased spatial resolution to determine critical local strain rates.

If we assume that snow is a linear, isotropic, viscous medium, then the creep equation can be written:

$$d_{ij} = 1/\eta \, [(1+\upsilon) \, \sigma_{ij} - \upsilon \, \sigma_{kk} \, \delta_{ij}]$$

where d_{ij} is the deformation tensor, η is the viscosity, υ is the viscous analog of Poisson's ratio, σ_{ij} is the stress tensor, and δ_{ij} is the Kronecker delta. Thermodynamic laws limit the range of Poisson's ratio to $-1 < \upsilon < 0.5$. From the creep equation it can be shown that in the neutral zone of a slab (where the velocity gradients can be ignored), the direction of creep depends on the slope angle and υ. This means that for a given slope, measurements of the direction can be used to calculate υ. Figure 3 shows the range of motion possible (shaded gray) when calculated for a slope inclined at 36°. When $\upsilon = 0.5$ the motion is slope parallel (incompressible material) and the direction of motion becomes closer to vertical as υ approaches -1.

Our measurements indicate that the direction of motion within new snow was often outside the range possible that is imposed by the assumptions of this model. The observed motion was often within a few degrees of vertical (represented by the motion of particle P in figure 3) which would require υ to be unrealistically large and negative. The results indicate that low density snow can not be described as a compressible viscous medium and modeled as a simple continuum.

We believe the anomalous behavior is caused by thermodynamic processes. The morphology of the micro-structure of new snow is often complex which results in a high surface area to volume ratio. Thermodynamic processes act to minimize the surface energy on a grain scale which causes the micro-structure to evolve so as to minimize the ratio of surface area to volume. These changes in micro-structure cause the bulk volume of the snowpack to decrease independently of gravity. The process is temperature dependent and the rate would accelerate in the presence of small amounts of liquid water which increase the rate of metamorphism and also form liquid bridges resulting in "capillary strain". If we assume that this thermodynamically induced strain (ε_{therm}) acts in series with the gravity induced deformation, the creep equation can be rewritten to include this term:

$$d_{ij} = 1/\eta \, [(1+\upsilon) \, \sigma_{ij} - \upsilon \, \sigma_{kk} \, \delta_{ij}] + \varepsilon_{therm}$$

In theory it is possible to determine values for ε_{therm} by measuring the deformation of snow with the same viscosity and Poisson's ratio on slopes of different angles. Further experiments are planned to investigate this phenomenon in more detail and to understand the implications of the strain.

Identifying and quantifying this anomalous deformation is one of the most important results from the study. Our measurements indicate that the strain induced by thermodynamic processes can have a significant impact on the deformation of low density snow. This has a number of implications for understanding compaction of snow and for understanding snow slope stability.

LIST OF PUBLICATIONS AND TECHNICAL REPORTS

Conway, H., and R. Benedict, 1992. Measurements of snow temperature during rain. *Proc. International Snow Science Workshop*, Breckenridge, Co. USA.

Conway, H., and C.F. Raymond, In press. Snow stability during rain. *J. Glaciol.*

Conway, H., and R. Benedict, In press. Infiltration of water into snow. *Water Resources Research.*

Conway, H., and R. Benedict, In prep. Insitu measurements of snow deformation. *Cold Regions Science and Technology.*

LIST OF PARTICIPATING SCIENTIFIC PERSONNEL

Charles F. Raymond, Professor of Geophysics
Howard Conway, Research Assistant Professor
Robert Benedict MS (Geophysics).

No degrees awarded during this period.

REPORT OF INVENTIONS

No inventions to report

The views, opinions, and/or findings contained in this report are those of the authors and should not be construed as an official Department of the Army position, policy, or decision, unless so designated by other documentation.

SNOW STABILITY DURING RAIN

(In Press, Journal of Glaciology)

H. Conway and C.F. Raymond

(Geophysics Program AK-50, University of Washington, Seattle, WA 98195, USA)

ABSTRACT

The mechanical response of snowpacks to penetrating liquid water was observed over two winter seasons in the Central Cascade Mountains, Washington, U.S.A. Following the onset of rain, three evolutionary regimes of snow behavior were identified: immediate avalanching, delayed avalanching, and return to stability. Immediate avalanching occurred within minutes to an hour after the onset of rain and the time of release could be predicted with an accuracy of less than an hour from meteorological forecasts of the transition from snow to rain. These avalanches usually slid on surfaces substantially deeper than the level to which water or associated thermal effects had penetrated. The mechanism by which alteration of a thin skin of surface snow can cause deep slab failure has not been identified, but several possibilities involving a redistribution of stress are discussed. Delayed avalanches released several hours after rain started. The delay varied, depending on the rate of increasing stress associated with the additional precipitation, and on the time taken for water to penetrate and weaken a potential sliding layer. It is difficult to accurately define the evolving distribution of liquid water in snow which makes it difficult to accurately predict the time of avalanching. Depth profiles of the rate of snow settlement showed that a wave of increased strain rate propagated into the snow in response to penetrating water. This type of measurement could prove useful for predicting when snow stability is reaching a critical condition. Avalanche activity was rare after continuation of rain for fifteen hours or more. This return to stability occurred after drainage structures had evolved and penetrated the full depth of the snowpack. Established drain channels route water away from potential sliding surfaces and are also relatively strong structures within a snowpack.

INTRODUCTION

Rain on snow is a major cause of mid-winter avalanches in maritime climates (Heywood, 1988; Conway and others, 1988) and spring avalanches caused by melt water are common (Ambach and Howorka, 1966; Kattelmann, 1984). Processes relating to the evolution of snow texture during wetting are well understood (Raymond and Tusima, 1979; Colbeck, 1986), and the weakening of snow from melting or rain is expected in terms of the grain-scale physics (Colbeck, 1982). However, it is still uncertain how macro-scale mechanical behavior of a snowpack is related to micro-scale processes. The response is complicated because of the layered stratigraphy of snowpacks (Colbeck, 1991) and also because liquid water does not penetrate snow uniformly (Wakahama, 1975; Colbeck, 1979, Marsh and Woo, 1984).

In this paper we discuss the effects of liquid water penetration on the evolution of snow texture and stratigraphy, and on the timing of avalanche release.

FIELD OBSERVATIONS

Concurrent observations of avalanche activity, snow properties and weather were made in the Cascade mountains near Snoqualmie Pass, Washington, U.S.A. during the winters of 1987-88 and 1988-89. Eight major rain on new snow events occurred during this period and accessory information is available from the local avalanche control effort that has been in operation since 1973.

The terrain near Snoqualmie Pass lies between 900 m and 1700 m and mid-winter rain is common at these elevations. A typical snowpack contains a relatively homogeneous base 2 to 3 m deep that has settled and grain-coarsened during one or more episodes of rain. Storms deposit up to 1 m of new snow and subsequent rain often causes some or all of the storm snow to avalanche.

Timing of avalanche cycles

The timing of avalanche activity during rain depends on the evolution of the mechanical properties of the snowpack which is partly controlled by the volume and rate of water influx. Figure 1a shows the number and timing of avalanche cycles in relation to the time that rain started and Figure 1b shows the amount of precipitation that had fallen as rain when each of the avalanche cycles occurred. The potential for avalanche release was highest a few minutes after rain started and before 1 mm of rain had accumulated. During continued rain, avalanche cycles occurred at various times up to thirteen hours after rain had started. After that time activity decreased indicating a return to stability. In all cases the return to stability occurred after less than 40 mm of rain had fallen on the snow.

Based on these observations we distinguish three types of behavior during rain on snow events: immediate avalanches which release minutes after rain starts; delayed avalanches which release more than one hour after rain starts; a return to stability which occurs ten to twenty hours after rain has started. Below we describe specific observations during rain on snow events.

Immediate avalanching

Hourly measurements starting on January 9, 1988, of air temperatures at 1160 m and 915 m, and precipitation at 915 m are shown in Figure 2. A temperature inversion occurred when a warm, westerly frontal system over-rode cold air trapped at the surface and this caused rain to start first at higher elevations and later at lower elevations. Avalanche activity began soon after rain started; avalanches released first at higher elevations and later at lower elevations (Fig.2). A snow profile near the lower starting zones two hours before the warm-up showed 18 cm of new snow (medium grain size, very low hardness) had been deposited on stratified, partly metamorphosed snow (well bonded and medium hardness). Deeper in the snowpack (40 cm below the surface) grains had coarsened during a previous wetting cycle and the snow hardness was high. One might expect loose snow avalanches soon after rain water had weakened snow near the surface and slab avalanches some time later after water had penetrated and weakened a sub-surface layer. However in this case the immediate avalanches were slabs 20 to 30 cm deep which slid on top of the well bonded, partly metamorphosed snow. In general, although some immediate avalanches released as loose slides, it was not uncommon for them to be slabs a few decimeters or more thick.

Delayed avalanching

Rain started at 13:00 on April 4, 1989 and many slabs up to 30 cm deep released *immediately* even although less than 0.25 mm of rain had accumulated (Fig.3). A second avalanche cycle occurred thirteen hours later on slopes which had not been controlled with explosives. The delayed avalanches were large (class 3+), wet slabs up to 1 m deep. Prior to the rain, a snow profile at a site several kilometers east of the major activity showed 11 cm of new snow (low hardness) which overlay layers of partly metamorphosed snow (medium hardness). A 2 cm layer of coarse, poorly bonded grains (low hardness) existed 52 cm below the surface. Grains deeper in the snowpack had coarsened from a previous rain event and were well bonded (high hardness). Although detailed fracture-line profiles are not available, avalanche technicians observed that only the recent new snow (low hardness) avalanched immediately, and the delayed avalanches slid on top of the old coarse grained snow.

During another storm shown in Figure 4, few avalanches released when rain started, but nine hours later several large (class 3) wet slabs up to 40 cm deep released on slopes which had not previously been controlled. This storm was on January 15, 1989 and although the air temperature had warmed eight hours before precipitation changed to rain at 17:00, it had remained below freezing. These conditions would allow the near surface snow to settle and gain strength and probably helped to minimize immediate activity. The sliding surface for the delayed avalanches was within the storm snow; snow deposited early in the storm had stabilized and did not avalanche.

Return to stability

An additional 63 mm of rain fell after the delayed avalanches on April 5 (Fig.3), but no avalanches released naturally. The snowpack was apparently stable after thirteen hours and 39 mm of water influx. The timing of the return to stability was not unique; thirteen hours is the longest time we have recorded. In other cases the snow stabilized more rapidly and after less liquid water influx. For example on January 15, 1989, no avalanches released after seven hours of rain and 21 mm of water influx (Fig.4), and on January 14, 1988, a return to stability occurred after eight hours and 34 mm of water (Fig.6).

A return to stability during continued rain has also been observed at Milford in New Zealand where avalanche activity usually decreases after about twenty hours of rain (Conway, 1990). We are not certain what volumes of water throughput are typically

required to achieve stability in that area, but both snow accumulation and rates of precipitation are typically higher than those at Snoqualmie Pass.

PENETRATION OF MOISTURE AND HEAT

Moisture and heat alter the shape and texture of grains which affect the mechanical properties of the snow. We tracked the progress of water through snow by spreading water soluble dye at the surface and then excavating snowpits at different times during rain events. In cases where the snow had been previously wetted, the dye usually penetrated the full depth of a snowpack (2 m or more) within a few minutes. However when rain fell on new snow, water penetrated only the upper 5 to 10 cm in the first hour. Penetration to greater depths began as "flow fingers" which were about 1 cm diam., and 2 to 20 cm apart. Soon after fingering began, water flowed preferentially through a few of the fingers which enlarged at the expense of others. The evolution of larger flow structures could take up to ten hours and by that time they were typically 20 to 30 cm diam., 0.5 to 2 m apart, and in many cases penetrated the full depth of the snowpack. The diameter of the channels continued to increase during additional rainfall and after 24 to 48 hours they had usually coalesced, which made the entire snowpack coarse-grained and relatively homogeneous.

The surface topography of the snow changed during water infiltration. Moisture in the snow increases the rate of densification and so snow within a channel settles faster than snow outside a channel which is dry. Undulations developed at the surface as a result of the differential settlement and their wavelength was determined by the spacing of the channels. When the channels enlarged the amplitude of the undulations decreased and the surface became smooth again when the snowpack was homogeneous.

Several processes feed back positively during the evolution of drain channels: In granular materials water flows preferentially along a path that is already wet. This tendency is enhanced further in snow because the presence of liquid water causes grain-growth which increases the permeability to water [illegible]; Undulations at the surface effectively route any surface water towards the hollows which feed into existing flow channels.

Water often flowed laterally through sub-surface layers as well as downward through vertical channels. Sub-surface lateral spreading of water usually occurred within layers that were initially low density snow or at stratigraphic boundaries where a fine-grained layer overlay coarse-grained snow. This is in contrast with a more common perception that water spreads across the upper surface of impermeable ice crusts (Perla and Martinelli, 1976). The permeability of ice is controlled by veins which exist at grain boundaries, and vein size increases rapidly as the ice temperature increases above -0.1°C (Langham, 1974, 1975). The temperature of ice in direct contact with liquid water will be close to 0°C and in our experience ice crusts had little effect on the downward percolation of water.

The temperature profile of a snowpack delineates zones at the melting point and the potential presence of liquid water. A three-dimensional array is required for a more complete picture of the temperature distribution and such measurements are planned for the future. In this study we obtained one-dimensional profiles by allowing a vertical line of thermistors to be buried by snowfalls. Figure 5 shows hourly measurements of precipitation, air and snow temperatures at 915 m. Measurements start on January 9, 1988 which is the same event described in Figure 2. Rain started at 20:00 when the air temperature increased above 0°C, but temperatures 24, 34 and 54 cm below the surface did not increase until four hours later at midnight (Fig.5). The slabs which released minutes after rain started were 20 to 30 cm deep and the temperature profile suggests that the avalanches released before water had penetrated to the sliding layer. It is possible that water did penetrate to the sliding layer through a channel and the signal was missed by the measurements, but there was no evidence of that happening.

Figure 6 shows other measurements of air temperature and snow temperatures 15, 25 and 40 cm below the surface. Rain started at 3:30 on January 14, 1988 and numerous slabs up to 40 cm deep avalanched immediately. Again the temperature profile suggests that water and associated thermal effects had penetrated less than 15 cm into the snow at the time of release. Seven hours later a second avalanche cycle occurred and by this time the thermal wave had penetrated at least 40 cm. We do not have a temperature profile at the starting zone which was about 100 m higher than the study site, but it is likely that liquid water had penetrated to the sliding surface by the time the delayed avalanches released. Avalanche activity decreased about eight hours after rain had started and before all the snow was at 0°C; apparently homogeneity of the snowpack is not a necessary condition for a return to stability during rain on snow events.

SETTLEMENT PROFILE

The rate of snow settlement is influenced by the additional weight of the rain as well as metamorphic processes associated with the penetration of moisture and heat. We expect the rate of settlement will increase when snow is first wetted and decrease as grains round and become closely packed. Depth profiles of settlement in a horizontal snowpack were obtained from the vertical velocity of shoes which were buried at different depths. Velocity was measured by running a cord vertically up from a shoe to a rotary potentiometer suspended above the snow surface. The system worked well except for some short-term disturbances caused by winds buffeting the cord which caused intervals of no apparent movement until the snow settled sufficiently to take up slack in the cord. The shoes, which were 8 cm square perforated plastic sheets, were set at the surface at different times during snow storms. This procedure minimized disturbances to the snow and to subsequent water percolation. Vertical strain rate was derived from velocity differences between shoes. The pattern of water infiltration causes differential settlement and so a three-dimensional array of shoes would offer a more complete picture. In our one-dimensional setup the shoes were not aligned directly above each other which complicates interpretation of the measurements because one shoe may respond to a local perturbation that does not affect a nearby shoe. Another limitation of the experimental procedure was that shoes were set manually at convenient times; it would be better to make measurements with closer depth resolution.

Figure 7 shows profiles of the vertical velocity and strain rate in a level snowpack starting on April 4, 1989. Very light rain started at 13:00 (less than 0.25 mm hr^{-1}) and at that time shoes were located at the surface, and also below the surface at depths of 18 cm and 38 cm. We have not smoothed these velocity profiles and we suspect that the short-term fluctuations in the velocity measurements at 38 cm reflect disturbances from wind or snow falling on the cord. The snow deeper than 38 cm had been soaked by rain during a previous warming and had grain-coarsened. Snow between 18 and 38 cm had partially settled but had not been wetted, and the most recent snow (0 - 18 cm) was low density (ρ = 70 kg m^{-3}). When rain started this recent snow settled rapidly (greater than 16 mm hr^{-1}), but velocities deeper in the snowpack (at 18 cm and 38 cm) remained less than 4 mm hr^{-1}. In fact the deeper shoes did not begin to show a mechanical response to the rain until eight hours later. The velocity at 18 cm reached a maximum of 8 mm hr^{-1} at 1:45 on April 5 (12.25 hours after rain started), and the velocity at 38 cm reached a maximum of 6 mm hr^{-1} at 2:45. The strain rate between 18 and 38 cm reached a maximum of about 0.02 hr^{-1} at 2:30 on April 5 which was thirteen hours after the onset of rain. Rates of settlement decreased after that and by 6:00 on April 5 (17 hours after rain had started), the strain rate at all depths was less than 0.005 hr^{-1}. Excavations at 9:00 on April 5 showed that all shoes were located within a channel where the snow had densified (ρ = 440-460 kg m^{-3}) and grain-coarsened (1-2 mm diam.). The snow surface topography was undulating with a wavelength of 1 to 1.5 m; between the channels the snow was still dry and fine-grained.

The evolution of snow stability during this storm was discussed earlier (Fig.3). The most recent snow (equivalent to the upper 18 cm at this site) avalanched immediately rain started. Thirteen hours later delayed avalanches slid to the depth of the coarse-grained snow (38 cm deep at this site), and then activity decreased. Although the avalanches started from zones where conditions may have been different from those at the study site, these three stages of mechanical evolution are evident in the settlement profile. Vertical strain rate was high at the snow surface during the initial instability, and high later at depth when the delayed avalanche cycle occurred. Strain rates were decreasing when observations indicated that avalanche activity had decreased.

About ten hours after rain started, the vertical velocity at 18 cm exceeded the velocity at the surface and this condition existed for the next five hours (Fig.7). This condition could be a result of differential settlement as discussed earlier or alternatively, the cohesion of the moist surface snow may have increased sufficiently to partially bridge the snow below. In other cases we have excavated snow beneath a moist surface layer and observed that the moist layer could often support itself over distances up to 1 m without sagging appreciably. We are not sure if bridging is important, but it is conceivable that stress generated during the collapse of a bridge could contribute to instability.

DISCUSSION

MECHANICAL RESPONSE OF SNOW TO RAIN

Immediate response

The potential for avalanche release is highest immediately after rain first falls on new snow. The avalanches are often slabs 30 to 50 cm deep and yet observations and measurements indicate that moisture and heat have penetrated only 5 to 10 cm into the

snow at the time of release. Changes at the surface must somehow alter the distribution of stress deeper in the snowpack and cause failure. This could occur in several ways:

- Gravitational loading. Precipitation rate in the area is usually less than 10 mm hr^{-1} which would increase the average down-slope shear stress on a 30° slope by about 50 Pa hr^{-1}. Locally the stress might increase more than this, but it is unlikely that all immediate avalanches release as a result of such small increases of average stress.

- Inertial loading. Small surface avalanches or snow falling from trees impose inertial loads that could cause deeper slab release. In some cases we have seen evidence of such disturbances but in many cases we have not.

- Redistribution of longitudinal stress. A loss of tensile strength over part of a slab could be significant in situations where the strength of the slab was critical for maintaining stability. A partial loss of strength could increase the tensile stress sufficiently to cause tensile failure of the remaining slab. For example a complete loss of strength in the upper 10 cm of a 30 cm slab could increase the longitudinal stress in the lower 20 cm by up to 50%. Water could weaken the surface of a slab by decreasing the strength of bonds between grains which relieves longitudinal stress by creep. Alternatively, high capillary forces active in moist snow could generate high tensile stress by pulling grains against boundary constraints. This stress would be transient but might be sufficient to cause tensile cracks which would decrease the strength of the moist surface snow. At this point we can not distinguish between these alternative mechanisms that might weaken the surface snow. Settlement of the snow would also decrease the cross section over which longitudinal force is supported and raise the stress. This process would probably result in a compensatory strengthening of the slab as it densified and would not necessarily destabilize a snowpack.

Observations suggest that immediate avalanching occurs only if the snow stability before rain is already close to critical. For example snowpacks that have had time to strengthen during a slow warm-up are less susceptible to immediate instability. In many cases a snowpack will not respond to artificial control before rain starts and yet it will avalanche naturally soon after the onset of rain (Wilbour, personal communication). It has been suggested that a potential slab avalanche contains zones of basal weakness and zones of basal pinning and that fracture can be initiated by a localized perturbation at a trigger zone (Conway and Abrahamson, 1984; Gubler and Bader, 1989). An explosion or a skier might impose a locally large perturbation but might miss a critical zone. Rain affects all the snow surface more or less simultaneously and although the amplitude of the perturbation may be small, it is far reaching and is likely to affect a critical zone if one does exist. The ubiquity of avalanches at the onset of rain implies that freshly deposited snow often contains at least one critical trigger zone which, when disturbed even at a low level, will initiate failure.

Delayed response

Stress evolves during continued rain as water adds weight to the snowpack and also penetrates and potentially weakens a sub-surface layer. It thought that a zone of basal weakness extending over a few meters or more is required to initiate slab failure, and this condition could develop when water spreads laterally along a sub-surface layer. Vertical penetration of water occurs through channels which are usually spaced less than 2 m apart, and this spacing would allow water to spread laterally over large basal areas almost simultaneously.

The presence of liquid water could weaken a snowpack in several ways:

- Water causes melting at grain boundaries and bonds which reduces friction between grains.

- Grains of new snow are often intricately shaped and the ratio of surface area to volume is large. Metamorphic processes are rapid in the presence of liquid water and grains change shape and texture rapidly. Although strength increases after grains have rounded and become closely packed. strength decreases during large textural changes. Further, we have observed a wave of increased rate of vertical strain which is associated with water penetrating into a horizontal snowpack. On slopes, vertical strain has a normal and a downslope shear component. A high rate of basal shear strain would contribute to instability (Gubler and Bader, 1989), and the slope normal component imposes a bending moment in the slab which may also contribute to instability.

Return to stability

Evidence from stratigraphic profiles, temperature profiles, and surface topography indicate that a return to stability occurs before the entire snowpack has become isothermal and homogeneous. Several factors contribute to increase stability during continued rainfall.

- Avalanching will usually stabilize the snowpack remaining but this is not a necessary condition; we have often observed slopes stabilize without avalanching.

- After drain channels have penetrated the full depth of a snowpack, subsequent water can pass directly through the snow and then it is less likely to accumulate and spread laterally at a sub-surface layer. Further, the snow within channels has densified which makes the structure relatively strong and the close spacing between channels interrupts the continuity of a potential shear layer. In most cases stability increases after drainage has been established, but in a few cases water might accumulate at the snow-ground interface and cause the release of full-depth avalanches.

AVALANCHE PREDICTION

The timing of avalanches that release immediately rain starts can be predicted by forecasting meteorological conditions in the avalanche starting zones. A network of weather stations surrounding the starting zones and located in the tracks of approaching storms offers a means of forecasting the onset of rain at a specific site.

Accurate prediction of delayed avalanches is more problematical. It is difficult to define the time of release without specific knowledge of the snow stratigraphy and how the evolving spatial distribution of liquid water will affect its strength. In our experience the delay varied up to thirteen hours after rain started but longer delays have been observed in situations when the snowpack was deep and had not been wetted previously (Breyfogle, personal communication).

CONCLUSIONS

Substantial depths of new snow often avalanche at the onset of rain. Evidence from stratigraphic, temperature and velocity profiles at that time indicate that these avalanches release before moisture or heat have penetrated more than a few centimeters into the snow. The release mechanism for this type avalanche does not require liquid water to penetrate and weaken a basal layer.

During continued rain the potential for avalanche release can remain high for ten to twenty hours. This type of instability is controlled by the stresses which evolve as a result of liquid water penetrating the snowpack. Water penetration occurs through vertical channels that occupy only a small part of the snowpack. Water is sometimes diverted from a vertical channel and may flow laterally through a sub-surface layer or along a stratigraphic boundary. The presence of water weakens a layer either by melting grain contacts or by causing rapid textural changes within the snow. Snow stability decreases when the strength of a basal layer decreases.

The length and diameter of channels increase with water influx and in time they penetrate the full depth of the snowpack. After drainage has been established, water is routed away from potential sliding surfaces and snow stability increases. Even during continued rain, avalanche release is rare after drainage through a snowpack has been established.

ACKNOWLEDGEMENTS

This research was supported by the U.S. Army Research Office and the Washington State Department of Transportation. Craig Wilbour, Steve Breyfogle, Lee Reddon and Joe Wilson (avalanche technicians at Snoqualmie Pass) assisted with the research.

REFERENCES

Ambach, W. and F. Howorka, 1965. Avalanche activity and free water content of snow at Obergugl. IASH Publ. 69, 65-72.

Gubler, H. and H.-P. Bader, 1989. A model of initial failure in slab avalanche release. Annals Glaciol., 13, 90-95.

Colbeck, S.C. 1979. Water flow through heterogeneous snow. Cold Reg. Sci. and Technol., 1(1),37-45.

Colbeck, S.C. 1982. An overview of seasonal snow metamorphism. Rev. Geophys. and Space Phys. 20(1), 45-61.

Colbeck, S.C. 1986. Statistics of coarsening in water-saturated snow. Acta Metall., 34(3), 347-352.

Colbeck, S.C. 1991. The layered character of snow covers. Reviews Geophys., 29(1), 81-86.

Conway, H., 1990. Review of avalanche program on SH 94, New Zealand. Technical report prepared for Transit New Zealand, Dunedin, New Zealand.

Conway, H., and J. Abrahamson, 1984. Snow stability index. J. Glaciol., 30(106), 321-327.

Conway, H., S. Breyfogle and C. Wilbour, 1988. Observations relating to wet snow stability. Proceedings International Snow Science Workshop, Whistler, 211-222.

Heywood, L. 1988. Rain on snow avalanche events - some observations. Proceedings International Snow Science Workshop, Whistler, 125-136.

Kattelmann, R.C. 1984. Wet slab instability. Proceedings International Snow Science Workshop, Aspen, Colorado, 102-108.

Langham. E.J. 1974. Phase equilibria of veins in polycrystalline ice. Can. J. Earth Sci., 11, 1280-1287.

Langham. E.J. 1975. The mechanism of rotting ice layers within a structured snowpack. IASH Publ. 114. 73-81.

Marsh, P. and M. Woo, 1984. Wetting front advance and freezing of meltwater within a snowcover. 1. Observations in the Canadian Arctic. Water Res. Res., 20, 1853-1864.

Perla, R.I. and M. Martinelli, 1976. Avalanche Handbook No.489, U.S. Dept. Agric. Forest Service, Fort Collins, Colorado.

Raymond, C.F. and Tusima, K. 1979. Grain coarsening of water-saturated snow. J.Glaciol., 22(86), 83-105.

Wakahama, G. 1975. The role of meltwater in densification processes of snow and firn. IASH Publ. 114, 66-72.

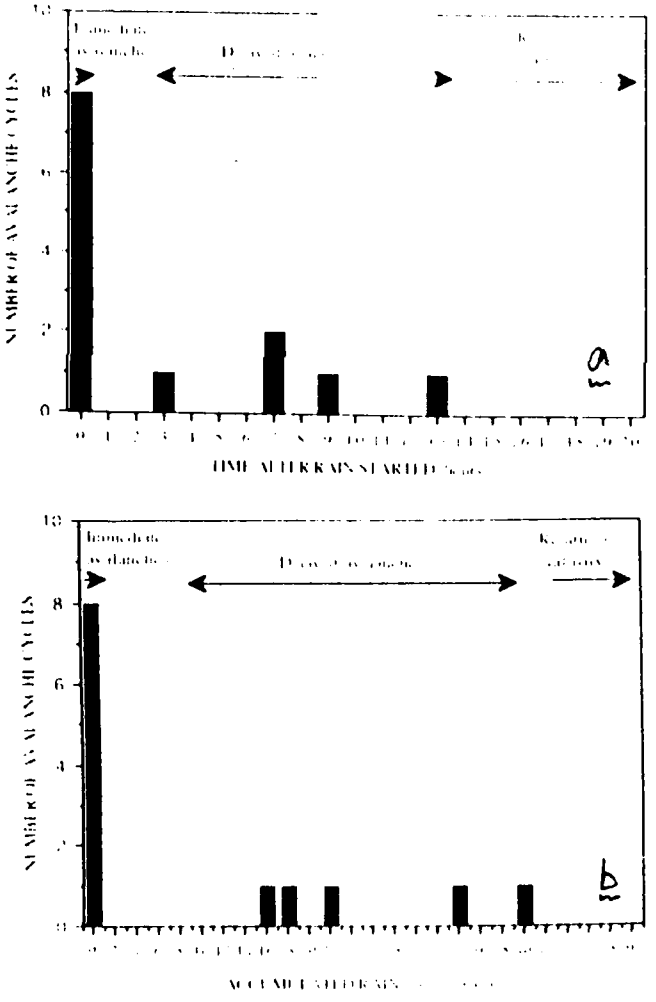

Fig. 1. a. The number and timing of avalanche cycles in relation to the time that rain started. b. The amount of precipitation that had fallen as rain when each of the avalanche cycles occurred. These data are from the eight rain-on-new-snow events that occurred during the winters of 1987-88 and 1988-89.

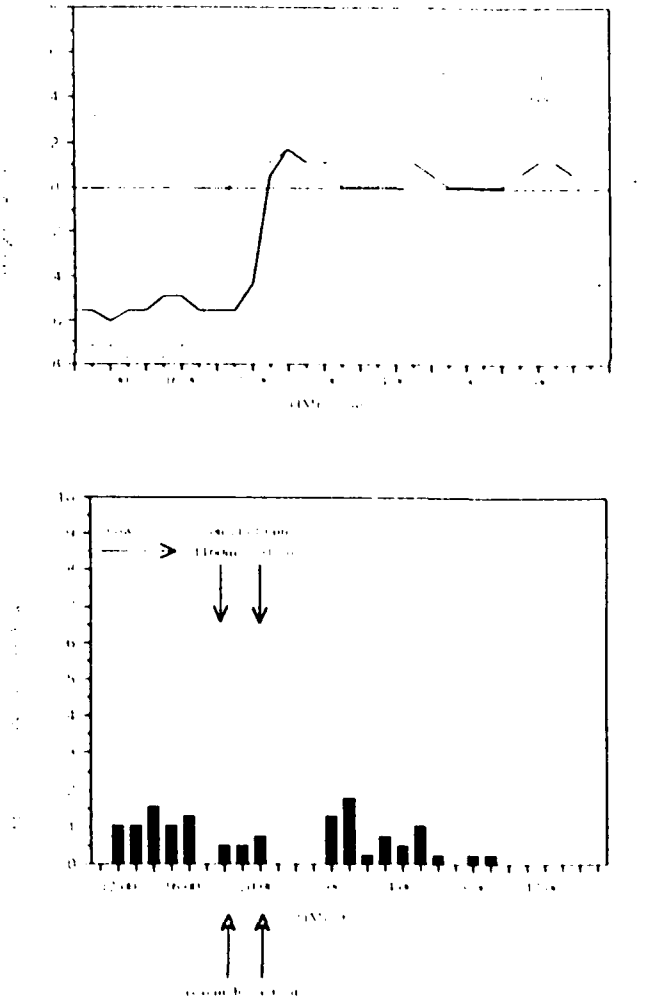

Fig. 2. Hourly measurements of air temperature at 915 and 1160 m and precipitation at 915 m starting at 1000 h 9 January 1988. Closed arrows show the timing of avalanche activity, starting first at high elevations (1100 m) where warming first started, and then two hours later at lower elevations (930 m). The timing follows the time that rain started at the respective starting zones.

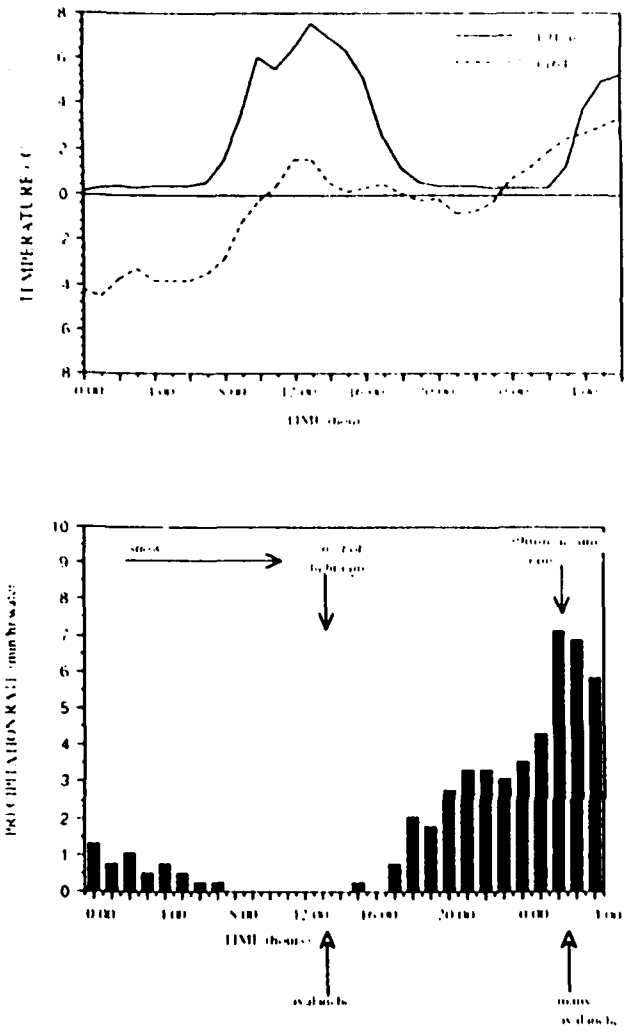

Fig. 3. Hourly measurements of air temperature at 915 and 1615 m and precipitation at 915 m starting at midnight on 4 April 1989. Closed arrows show timing of avalanche activity that occurred first when precipitation changed to rain, and again 13 hours later.

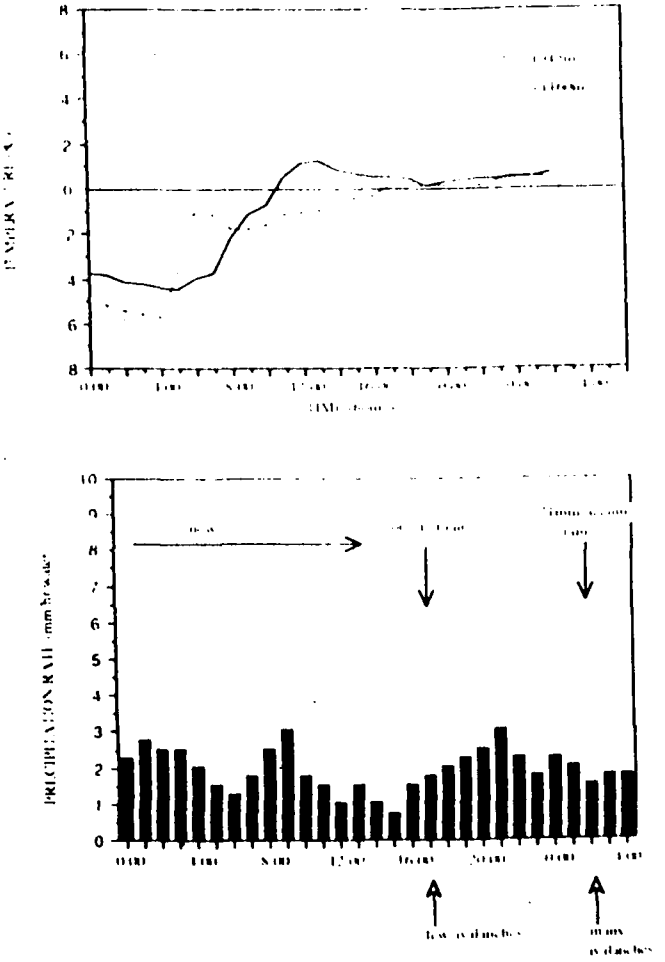

Fig. 4. Hourly measurements of air temperature at 915 and 1160 m and precipitation at 915 m starting at midnight on 14 January 1989. Closed arrows show timing of minor avalanche activity that occurred as precipitation changed to rain, and major avalanche activity nine hours later.

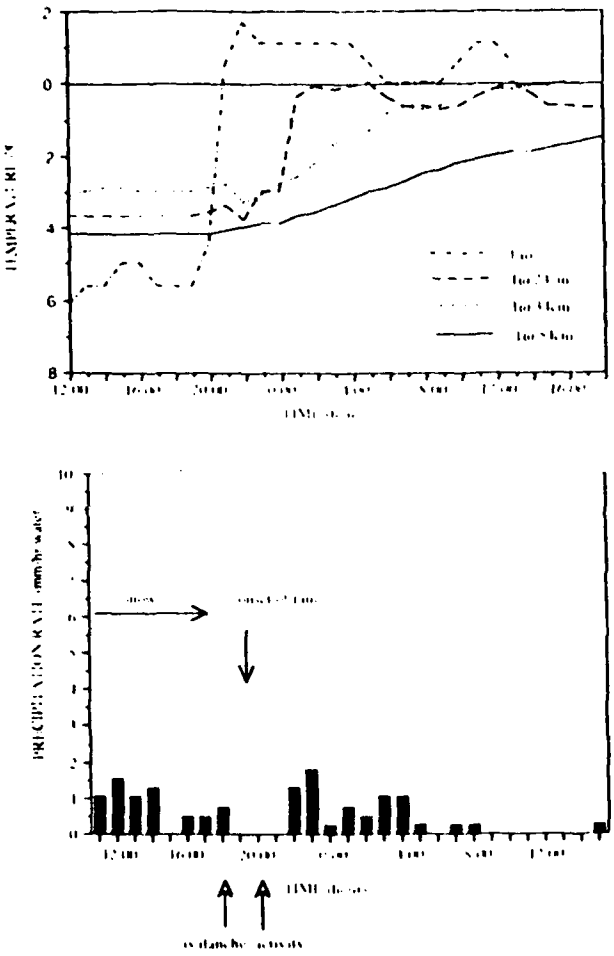

Fig. 5. Hourly measurements at 915 m of air and snow temperatures and precipitation starting at noon on 9 January 1988. Thermistors were buried 24, 34 and 54 cm below the surface. Major avalanche activity (marked by the closed arrow) occurred at the onset of rain but snow temperatures did not warm significantly until about four hours later.

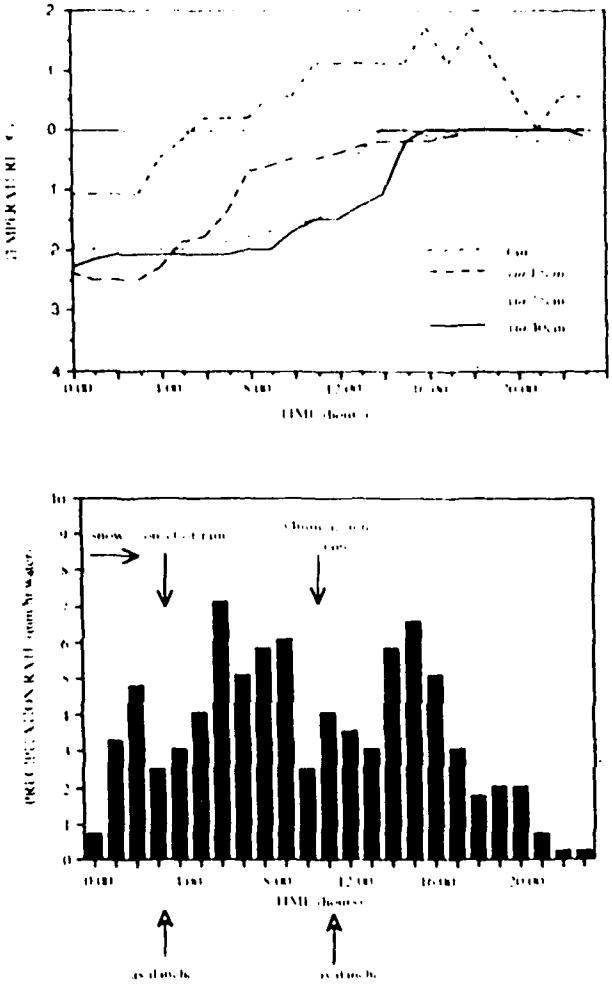

Fig. 6. Hourly measurements at 915 m of air and snow temperatures and precipitation starting at midnight on 14 January 1988. Thermistors were buried 15, 25 and 40 cm below the surface. Closed arrows mark the timing of avalanche activity which occurred at the onset of rain, and again eight hours later. Snow temperatures were well below freezing when avalanches first released, but warming had started when the second avalanche cycle occurred.

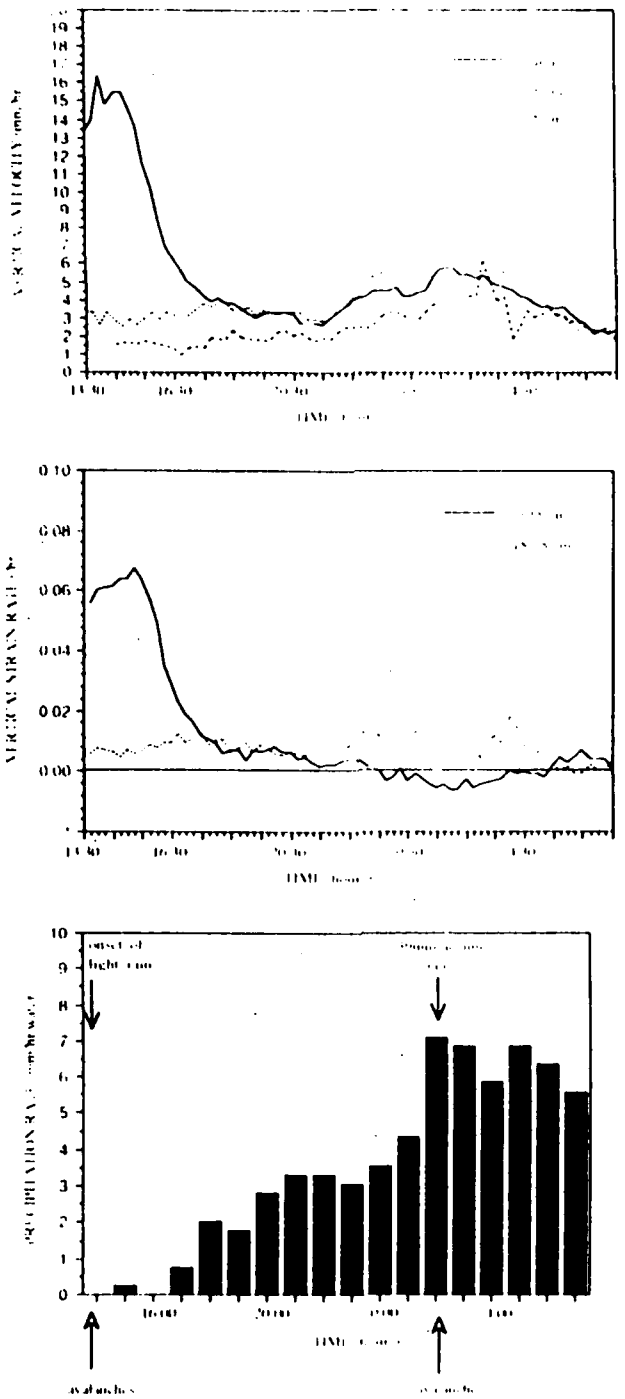

Fig. 7. Vertical velocity, strain-rate and precipitation measurements made in a level snowpack during 4–5 April 1989. Velocity and strain-rate measurements were obtained from shoes at the surface, and below the surface at 18 m and 38 cm. Closed arrows show the timing of avalanche activity that occurred first when precipitation changed to rain and again 13 hours later.

WATER RESOURCES RESEARCH, VOL. ?, NO. ?, PAGES ?-?, MONTH 1994

Infiltration of water into snow

H. Conway and R. Benedict

Graduate Program in Geophysics, University of Washington, Seattle

Abstract. Measurements from a rectangular grid of thermistors set in a maritime snowpack are used to study the infiltration of water during two midwinter rain on snow events. The progress of wetting is tracked in real time by monitoring changes in the position of the zero-degree isotherm. Rates and patterns of infiltration are calculated for each event. Infiltration was not uniform, and water penetrated through localized channels that often occupied less than 50% of the total volume of the snowpack. The evolution of wetting was strongly influenced by the snow stratigraphy. In one case the snowpack contained multiple ice layers, and vertical flow was impeded and diverted laterally for several hours at each layer. In the other case the snowpack was more homogeneous, and water concentrated in channels and penetrated to depth more rapidly. The measurements of temperature are also used to calculate the components of heat transfer within the snow during each rain event. Heat transfer in dry snow occurs primarily by conduction, and rates are relatively slow. However, introduction of liquid water results in the release of latent heat when water freezes on contact with subfreezing snow at the wetting front. The release of latent heat dominates heat transfer and has the potential to warm the snowpack rapidly. Rates of freezing needed to satisfy the heat equation are calculated. In both cases studied, less than 4% of the total influx of rainwater needed to change phase. Most of the rain remained liquid and wet the snow or drained through the snowpack.

act must para-

Introduction

Warming or introduction of liquid water into snow alters the texture which impacts the hydraulic properties and strength of snowpacks. It is of interest to understand the details and timing of warming and infiltration in order to improve models of snow hydrology and snow stability. Knowledge of the spatial pattern of wetting and the rate of vertical penetration is of particular interest in maritime climates where midwinter warming and rain are common causes of avalanche release [*Conway and Raymond*, 1993].

Numerous studies of infiltration into natural snowpacks have been made by spreading water soluble dye at the snow surface and examining the end conditions by excavating snow pits after rain and mapping the presence of the dye. It is well known that water penetrates previously dry snow through channels that occupy only a fraction of the total snow volume and that the local rate of penetration is often much faster than average rates [e.g., *Gerdel*, 1954; *Wakahama*, 1975; *Colbeck*, 1979; *Marsh and Woo*, 1984, 1985; *Kattelmann*, 1985, 1989].

Relatively few studies have been made in real time because instruments that are available (e.g., lysimeters and tensiometers) are difficult to use in subfreezing snow. Further, these instruments need to be set in the wall of a snow pit, and the excavations potentially alter the thermal and hydrological properties of the snowpack. Recently, *Sturm and Holmgren* [1993] installed heat flux transducers at the base of a subfreezing snowpack. The transducers produced a characteristic signal when hit by water which they used to detect the arrival of water at ground interface. They suggested that an array of transducers set within snowpacks would offer a means to study infiltration in real time.

Here we use measurements of snow temperature to track infiltration. The temperature measurements are used to calculate rates of heat transfer and rates of freezing during infiltration, and we combine these calculations with measurements of rainfall to estimate the average moisture content of the snowpack.

Paper number 93WR03247.
0043-1397/94/93WR-03247$05.00

Physical Processes

During infiltration the snowpack is composed of zones that are wet and zones that are dry, and these are separated by a zone of transition or "wetting front." Processes that occur within each zone have been described by *Pfeffer et al.* [1990] and the following observations generally apply:

1. In dry regions the snow is subfreezing, and there is no flux of liquid water. Heat transfer occurs mainly by conduction and is driven by the divergence of temperature gradients.

2. Snow in wet regions is considered to be isothermal and near 0°C. Although small temperature gradients exist across grain boundaries in wet snow [*Raymond and Tusima*, 1979], on a macroscale these cancel out, and the net heat transfer is small. Liquid water in wet zones becomes mobile only after the water content has increased sufficiently to form a continuous film through the pore spaces [*Colbeck*, 1979]. This critical moisture content is known as the "irreducible" moisture content and is strongly dependent on the size and texture of grains [*Wankiewicz*, 1979].

3. Some liquid water arriving at the wetting front freezes on contact with subfreezing snow, and latent heat released during the phase change warms the snow to near 0°C. The heat and the water equations are coupled by this process.

Below we discuss the equations describing the heat and liquid water balance further and use measurements to calculate the fluxes of heat and liquid water during infiltration.

Heat Flux

In dry snow it is usual to combine the effects of conduction and vapor transfer and define an effective thermal conductivity (K_{es}). Numerous empirical relationships have been proposed for K_{es}, and we have used one from *Yen* [1981]:

$$K_{es} = 2.22\rho_s^{1.88} \tag{1}$$

where ρ_s is the density of snow in megagrams per cubic meter.

The flux of sensible heat at any point in the snowpack can be separated into a conductive component and a nonconductive component (δQ) which is either a heat source (positive) or a heat sink (negative). The general heat equation at a point can be written

$$C_s\rho_s \frac{\partial T}{\partial t} = \nabla \cdot (k\nabla T) + \partial Q \tag{2}$$

where T is the snow temperature, C_s is the bulk heat capacity of the snow, and t is time.

When water freezes on contact with subfreezing snow at the wetting front, the nonconductive term is dominated by the latent heat released. In this case the heat source (δQ_f) associated with freezing is

$$\partial Q_f = L_f \frac{\partial m_f}{\partial t} \tag{3}$$

where L_f is the latent heat of fusion, and $\partial m_f/\partial t$ is the mass rate of freezing per unit volume.

Liquid Water Flux

The general equation for continuity of liquid water in the snowpack is

$$\frac{\partial \theta_s}{\partial t} = -\nabla \cdot \mathbf{q} + \partial F \tag{4}$$

where θ_s is the volumetric moisture content of the wetted snow, $\mathbf{q}$ is the volumetric flux vector of liquid water, and δF is the source or sink of liquid water.

The volume loss of liquid water due to freeze-on (δF_f) is

$$\partial F_f = \frac{1}{\rho_w} \frac{\partial m_f}{\partial t} \tag{5}$$

where ρ_w is the density of water.

After the snowpack has become isothermal we do not expect any further loss of liquid water until it drains from the snowpack. On the other hand, there is a possibility of meltwater production from snowmelt.

Methods

Instrumentation

Temperature profiles were measured in a horizontal snowpack at an elevation of 915 m in the Cascade Mountains near Snoqualmie Pass, Washington, during the winter of 1991–1992. Midwinter rain is common at these elevations. Measurements were made at 15-min intervals using up to 110 thermistors (Thermometrics P100DA202M) multiplexed to a data logger. The thermistors had been potted in white heat-shrink tubing and white epoxy to make them waterproof and to minimize heating from penetrating solar radiation. We are primarily interested in temperature gradients rather than absolute temperatures, and each thermistor was field calibrated at the melting point for seasonal snow. Calibration was achieved at a time when the snow surrounding the thermistor was saturated and the electrical resistance of the thermistor had stabilized at a constant value. The temperature of wet snow is likely to be slightly less than 0°C, but we assigned this temperature to be the "zero curtain" or "zero point." The resolution of measurements at this temperature was better than ±0.01°C.

The thermistors were arranged in a vertical rectangular grid 1.5 m wide and up to 2 m deep (see Figure 1). To minimize disturbances to the snowpack the array was established by placing horizontal strings of thermistors sequentially at the surface as snow accumulated. Each string consisted of 11 thermistors spaced 15 cm apart. A parallel horizontal string set at the same height 1 m away supported the leads from the thermistor beads to the multiplexer (Figure 1). Although the technique minimized the possibility of introducing vertical thermal or hydraulic connections between thermistors, it did not preclude the possibility of introducing lateral connections. Initially, the vertical spacing between strings was about 15 cm, but the strings were free to settle with the snowpack and the spacing decreased with time. The spacing between thermistor strings was calculated from measurements of snow settlement. A profile of settlement was obtained by measuring movement of markers buried at different depths within the snowpack at 15-min intervals. More details of the snow settlement measurements and of the experimental setup have been described elsewhere [*Conway and Benedict*, 1992].

Rates of snow accumulation were measured manually and also by using a sonic ranger mounted above the snow surface. The water equivalent of the precipitation was measured using a shielded, heated tipping bucket gauge.

Interpretation of Measurements

The temperature measurements are two dimensional in a vertical plane, and we make a number of assumptions to facilitate interpretation of the measurements. The assumptions include the following:

1. The 0°C isotherm defines the position of the wetting front, and snow at 0°C contains liquid water. This assumption is reasonable given that the time to reach thermal equilibrium is expected to be less than a second [*Pfeffer et al.*, 1990], which is more than 3 orders of magnitude faster than the time interval between our measurements.
2. The section measured is representative of thermal and wetting conditions in the rest of the snowpack; although other cross sections might differ in detail, the overall pattern is assumed to be similar.
3. The distance between horizontal strings of thermistors is assumed to remain constant over the entire length of the strings. This may not always be correct because each string is free to deform with the snowpack, and snow usually settles differentially during infiltration [*Wakahama*, 1975].
4. To interpret the distribution of liquid water in the snowpack we assume that each thermistor defines the tem-

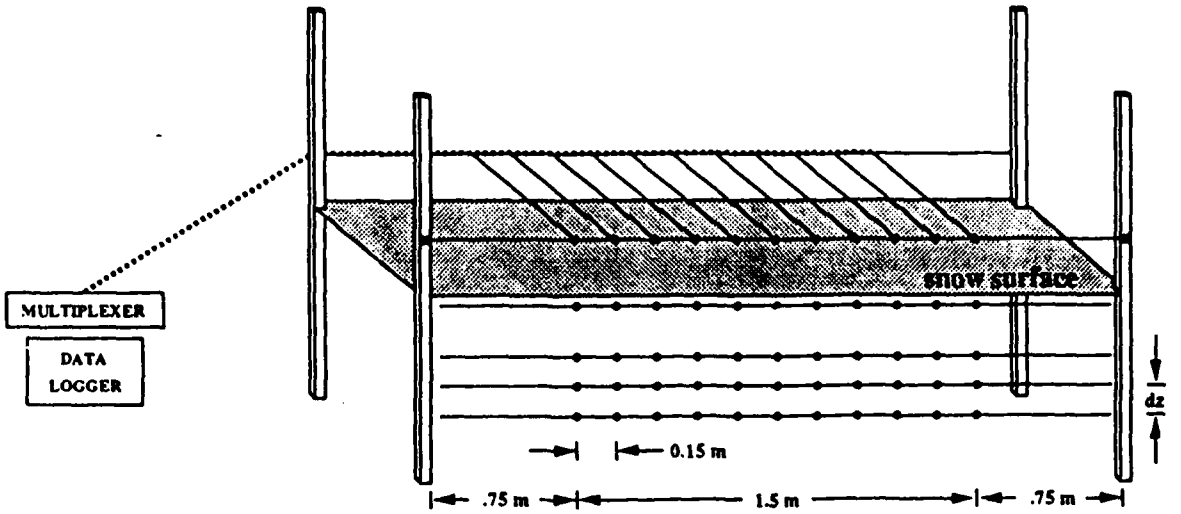

Figure 1. Setup of five of the ten strings of thermistors used during the 1991–1992 winter. In this illustration, string 5 is still suspended between the posts above the snow surface. Strings 1 to 4 had been released from the posts as they were buried by new snowfall. The vertical spacing between thermistor strings (δz) started at approximately 15 cm, but this distance decreased as the snowpack compacted.

perature of an area of surrounding snow. This area is rectangular, and its boundaries bisect the line segments connecting each thermistor and its nearest vertical and horizontal neighbors. In reality the temperature gradient between adjacent thermistors would be continuous, but here we want to maintain a simple representation of infiltration.

Case Studies

Two time series of vertical profiles of snow temperature are shown in Figure 2. The series were made during rain events, and the time of each profile is referenced to the onset of rain. To visually interpret infiltration we have binned the measurements of temperature into ranges that are represented by a gray scale. Temperatures at 0 ± 0.01°C (the accuracy of our measurements) are shaded black; we assume that liquid water exists in the snow at these temperatures. Temperatures between -0.01°C and -0.2°C are shaded gray, and temperatures colder than -0.2°C are white. For each event the snow stratigraphy before rain is described beside the first temperature profile. The stratigraphy is recorded according to the international classification for seasonal snow on the ground [*Colbeck et al.*, 1990]: 1b are new, 1-mm size, needlelike grains; 2a are 0.1 mm, partly rounded grains; 3a are 0.1–0.5 mm, rounded grains; 6a are 1.0 mm, rounded clustered grains; 8a is an ice layer. Once infiltration started it was more difficult to define the stratigraphy because textural changes are rapid in the presence of liquid water [*Raymond and Tusima*, 1979], and this is further complicated because the distribution of water through snowpacks is not usually uniform.

Below we discuss details of the two events:

Rain Event on January 15–16, 1992

Figure 2a shows the evolution of thermal conditions on January 15–16, 1992. Before rain started the snowpack contained two ice crusts. The crust 15 cm below the surface was 0.5 cm thick, while the crust 35 cm below the surface was 1 cm thick. The snow between these crusts was mainly fine grained. Air temperatures had warmed above freezing several hours before rain started at 2100 hours, which had warmed several of the subsurface thermistors (located 6 cm below the surface) to 0°C. At the onset of rain the average temperature of the snowpack was -0.9°C. The rain lasted for 10 hours, and a total of 19 mm of rain fell during that period.

Temperatures measured 1 hour after rain started show two zones where the zero-degree isotherm extended from the surface down to the first ice crust (Figure 2a). We interpret these zones to be channels where liquid water was concentrated. The third profile in the series (2 hours after the onset of rain) shows that vertical flow of water was still impeded at the first ice crust, and water had flowed laterally rather than vertically. In fact, water did not penetrate the upper crust until 4 hours after rain started, at which time almost all of the snow above the crust had been wetted. Once water did penetrate the upper crust the wetting front advanced to the next ice layer 20 cm deeper in the profile in less than 15 min. However, vertical penetration was stopped at the lower ice layer, and for the next 11 hours water again flowed laterally rather than vertically and had still not penetrated the lower ice layer when rain ceased. This "step and fill" pattern of infiltration was typical in layered snowpacks.

The profile 5 hours after rain started shows that two thermistors at the ice layer warmed to 0°C before the adjacent thermistors nearer the surface had warmed (see Figure 2a). A channel must have formed in such a way that water flowed past the upper thermistors without hitting them.

Rain Event on January 22–23, 1992

Figure 2b shows the evolution of thermal conditions during a second rain event starting on January 22. Cold weather between January 16 and 22 resulted in the formation of a thin crust at the snow surface. Precipitation started as snow, and when rain started at 1900 hours on January 22, 15 cm of new snow had accumulated on top of the crust, and the

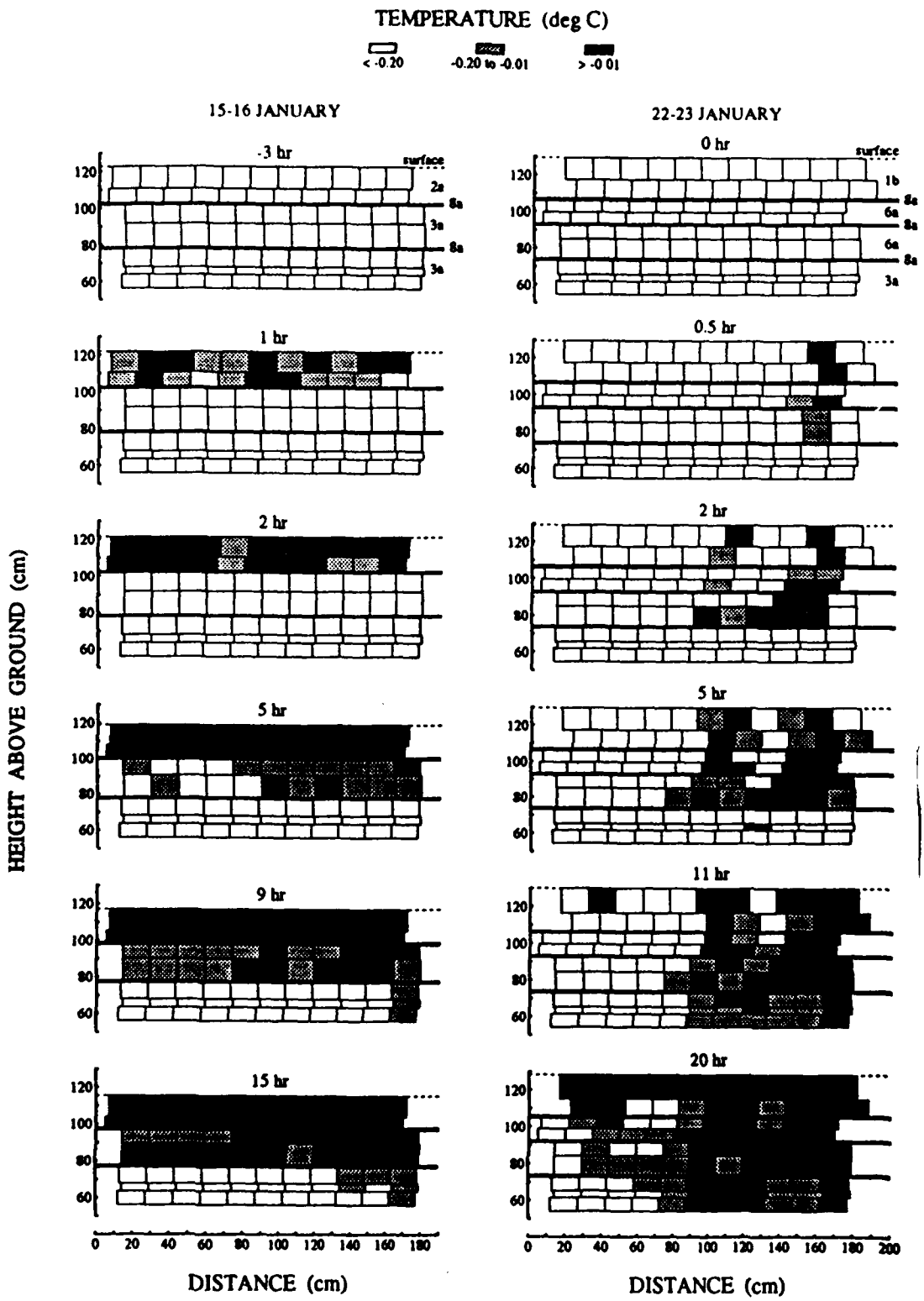

Figure 2. Vertical profiles of snow temperature during two rain events in 1992. The time written above each profile refers to the time after the onset of rain. Temperatures have been binned into ranges that are represented by a gray scale. Temperatures at 0 ± 0.01°C are shaded black; we assume that liquid water exists in the snow at these temperatures. Snow stratigraphy before rain is shown to the right of the first profile for each event. Stratigraphy is recorded according to the international classification for seasonal snow on the ground: 1b are 1 mm size, new, needlelike grains; 2a are 0.1 mm, partly rounded grains; 3a are 0.1–0.5 mm, rounded grains; 6a are 1.0 mm, rounded clustered grains; 8a is an ice layer.

upper thermistor string was buried 5 cm below the surface. The average temperature of the snowpack just before rain

started was −1.8°C. Rain lasted for 36 hours, and during that period a total of 100 mm of rain fell.

In this case water penetrated the new snow and the upper two ice crusts rapidly to reach the third crust (previously 35 cm but now 50 cm below the surface) in less than 30 min. However, vertical flow was impeded at that crust for the next 4 hours. During that time a second vertical channel developed, and some water was diverted laterally. After water penetrated the crust it continued to flow laterally as well as vertically, and the two vertical channels eventually merged to form a single, wide channel. Water penetrated beyond the lowest string of thermistors 11 hours after rain started, which made it impossible to track the maximum depth of infiltration. We suspect that water drained out the bottom of the snowpack soon after that time. Drainage occurred when less than 50% of the snowpack had been wetted. Water was slow to spread laterally from the main vertical channel, and the snowpack did not become completely isothermal until 40 hours after rain had started.

Evolution of Thermal Conditions

Figure 3 shows an example of the evolution of thermal conditions at 15-min intervals during infiltration at a grid point (x,z) located within the snowpack. The spatial configuration and relative positions of the thermistors are also indicated. In the example shown in Figure 3a, $T_{x,z+1}$ is the temperature measured at the thermistor located in the top row, second from the right in the profiles shown in Figure 2b during January 22–23. Rain started at 0 hours, and less than 15 min later the thermistor nearest the surface ($T_{x,z+1}$) warmed rapidly to 0°C. The temperature directly below and 18 cm beneath the surface ($T_{x,z}$) reached 0°C within 30 min, but adjacent thermistors at the same depth ($T_{x+1,z}$ and $T_{x-1,z}$) warmed to 0°C more slowly. These thermistors were not hit directly by the first pulse of water, and the flow channel did not expand laterally at this location until 6 or 7 hours later.

The rate of warming at $T_{x,z}$ is too fast to be explained by conduction alone, and we calculate the nonconductive component by solving for δQ from the heat equation (2). The partial derivatives are replaced with finite differences, and we use a Crank-Nicholson scheme [*Press et al.*, 1986] to calculate the flux divergence in two dimensions. Calculations are made over 15-min-time interval steps. Measurements from the settlement profile were used to calculate the z positions as well as the snow density at each time step. Snow density increases with settlement which impacts the calculation of thermal conductivity (1) and the calculation of the sensible heat flux (2).

The evolution of both the conductive and the nonconductive components of the sensible heat transferred at $T_{x,z}$ is shown at 15-min intervals in Figure 3b. Before rain started the rate of sensible heat transferred in the dry snow was less than 0.04 MJ m^{-3} h^{-1}. The thermal conditions at that time were typical of those described earlier for dry zones where heat transfer occurs primarily by conduction through the ice framework. Conditions changed significantly when rain started and water infiltrated the snow. A large nonconductive heat source (more than 4 MJ m^{-3} h^{-1}) dominated the heat transfer process for one 15-min interval. We attribute this large energy source to the release of latent heat as a result of freezing at the wetting front. The snow warmed rapidly, and the heat flux decreased to less than 0.2 MJ m^{-3} h^{-1} within an hour. During that time the conductive flux at the x,z location was negative (see Figure 3b) because the snow deeper and to the sides of the grid point was relatively cold. After 6 or 7 hours the temperature of the snow surrounding the x,z position reached 0°C, and the net heat transfer decreased to near zero.

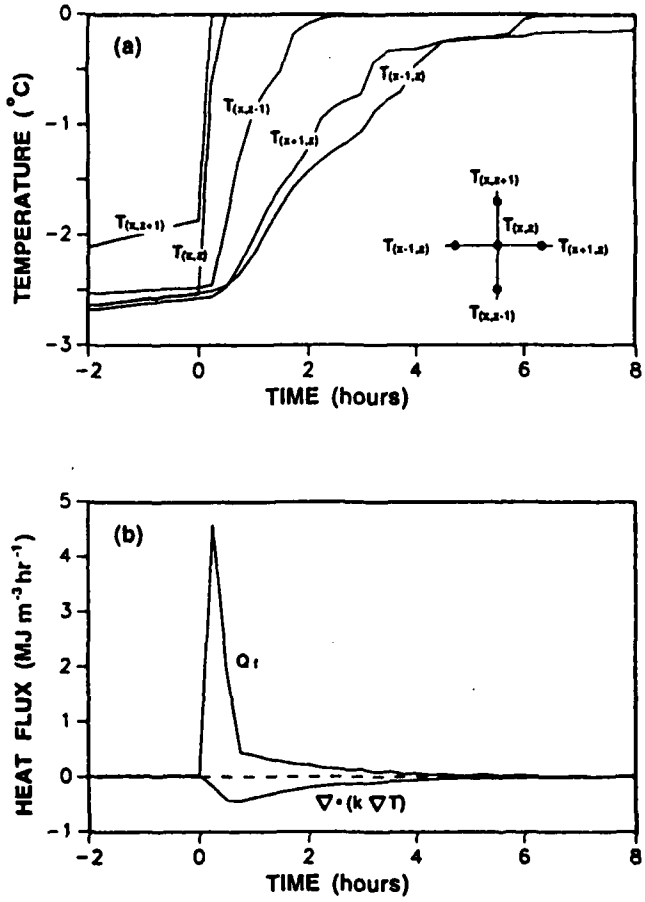

Figure 3. Evolution of thermal conditions during wetting. Rain started at 0 hours. (a) Snow temperature measurements at five locations during rain on January 22–23. Measurements were made at 15-min intervals, and the spatial configuration of the thermistors is shown. In this example, $T_{x,z+1}$ is the temperature measured at the thermistor located in the top row, second from the right, shown in Figure 2b. (b) The conductive and nonconductive components of sensible heat transfer at location x,z. The large heat source δQ_f at the onset of rain is attributed to latent heat released at the wetting front.

Calculations made in the same way at most other grid points show similar characteristics, although the timing of the latent heat source varied depending on the arrival time of the wetting front. At a few locations there was a transient heat sink during infiltration. This energy sink was not caused by cooling at the grid point (as might be expected if latent heat was absorbed due to melting) but rather because the surrounding snow had warmed to 0°C while the snow at the x,z position remained subzero. This scenario was discussed earlier (during infiltration on January 15) when we observed that water had apparently flowed past a thermistor, and zones deeper in the snowpack had warmed first. This situa-

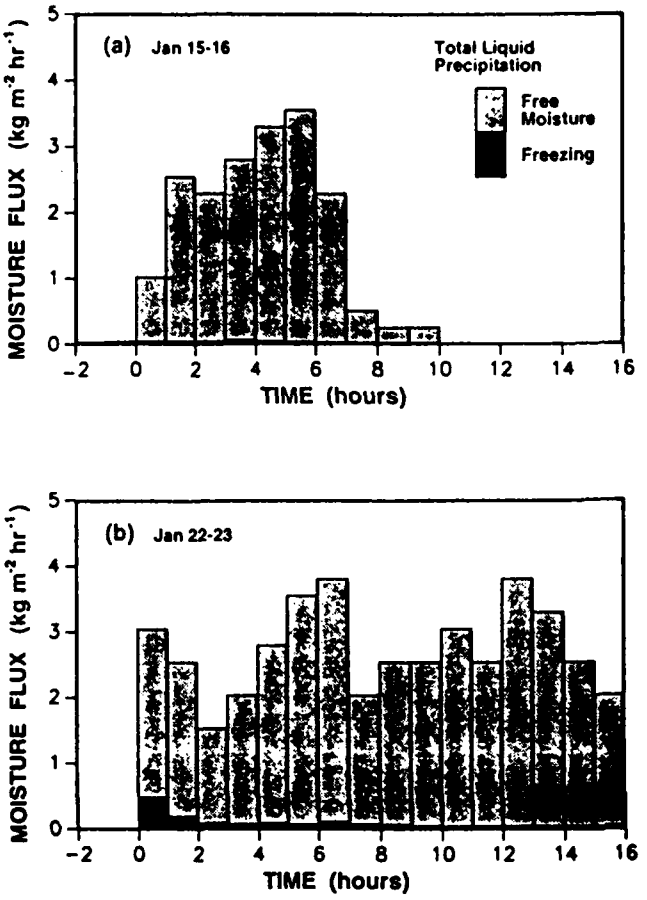

Figure 4. Evolution of moisture fluxes during wetting. Rain started at 0 hours, and each bar represents the total influx of rainwater during that hour. Some of the rain freezes (areas shaded black), while the remainder exists as free water (areas shaded gray). (a) Moisture fluxes on January 15–16. Before rain started the average temperature of the snowpack was −0.9°C. On average, less than 2% of the rainwater froze. (b) Moisture fluxes on January 22–23. Before rain started the average temperature of the snowpack was −1.8°C. About 17% of the rain froze during the first hour, but the fraction decreased as wetting progressed. On average, less than 4% of the rainwater froze.

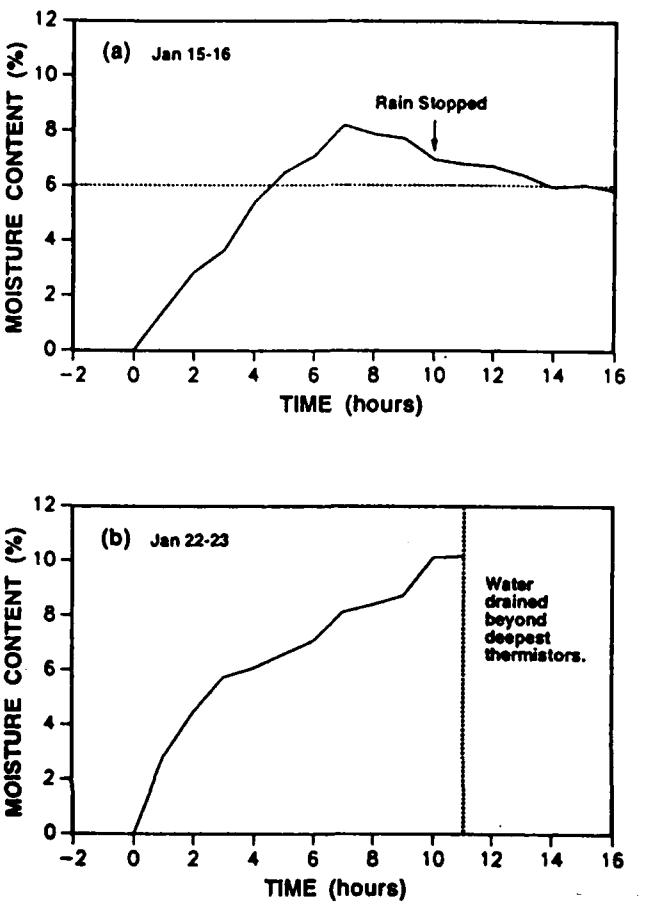

Figure 5. Evolution of moisture content of the wetted snow. (a) Moisture content on January 15–16. The moisture content reached a maximum of 8% during rainfall. Rain stopped after 10 hours, but water continued to infiltrate the snowpack until the moisture content decreased to a residual of 6%. (b) Moisture content on January 22–23. The moisture content reached a maximum of 10% about 11 hours after rain started. We are unable to estimate the moisture content after that time because water drained beyond the deepest thermistor, and the rate of drainage is not known.

tion is not unexpected given that the array of thermistors was two dimensional but infiltration is three dimensional.

At each time step we calculate the average nonconductive heat source for the entire snowpack by integrating the calculations at each grid point. The general characteristics of the integrated time series were similar, although the peak heat flux was slightly less than that shown in Figure 3b. If we assume that all of the nonconductive heat was caused by latent heat released during freezing, (5) can be used to calculate the average rate of freezing needed to satisfy the heat equation during each time step.

Liquid Water Balance

Average rates of freezing are subtracted from the rate of liquid precipitation to estimate the flux of liquid water through the snow. Figure 4a shows rates of precipitation and rates of freezing at 15 min intervals during the rain event that started on January 15. The rate of freezing necessary to rain started, and the rate decreased further as wetting continued. On average, less than 2% of the rainwater froze during this storm. Figure 4b shows conditions during rain on January 22. In this case the rate of freezing during the first hour was 0.5 kg m^{-2} h^{-1} which is about 16% of the precipitation rate at that time. However, the fraction decreased rapidly as wetting progressed, and on average, less than 4% of the rain needed to freeze in order to satisfy the heat equation.

We use these calculations in the liquid water equation (4) to estimate the average moisture content of the wetted portion of the snowpack. Because the cross section is two dimensional, the areas wetted are per unit length (in the horizontal y direction). Although there is considerable lateral movement of water in snowpacks, we assume that the net lateral fluxes are small and can be ignored. Further, we assume that water does not drain from the snowpack until the 0°C isotherm reaches the bottom of the array.

Figure 5 shows the evolution of the moisture content of

January 15–16 the moisture content increased to a maximum of 8% about 7 hours after rain started (see Figure 5a). The precipitation rate decreased after that time, and although rain stopped after 10 hours, wetting of previously dry snow continued until the moisture content decreased to about 6% by volume. Although slow drainage probably continued, we interpret this to be close to the irreducible water content of the snow. The value is somewhat higher than 3%, which is the value usually cited [*Colbeck et al.*, 1990], but it is not unreasonable given that moisture content depends strongly on snow texture. Figure 5b shows the evolution of moisture content during January 22–23. Water penetrated beyond the deepest thermistor string after 11 hours, and we are unable to estimate the moisture content after that time. However, just before drainage the moisture content was about 10%, which is closely similar to the maximum calculated during the first event.

The calculations of moisture content are particularly sensitive to uncertainties at the time of first wetting but become less sensitive as wetting proceeds. For example, we assumed that the entire box surrounding a thermistor was wet when its temperature reached −0.01°C, but in reality only a fraction of the area may have been wet because of its geometric configuration in relation to the thermistor. On the other hand, it is possible that part of the box was already wet before the thermistor reached −0.01°C. An underestimate of the initial wetted volume would overestimate the moisture content. Errors in the moisture content could also arise from uncertainties in the rate of liquid precipitation. Precipitation was often mixed rain and snow, especially at the onset of rain, but the gauge measured the water equivalent of all precipitation. Uncertainties arise because we had to rely on visual observations and measurements of air temperature to estimate the fraction of liquid precipitation.

Discussion of Measurements

Thermal Conditions During Infiltration

Here we have analyzed the evolution of thermal conditions within the snowpack during infiltration, and we do not attempt a complete energy balance. Energy transferred near the surface by longwave and shortwave radiation, turbulent exchanges, or from the heat capacity of warm rain could contribute to subsurface warming and influence the flux of liquid water through the snowpack. Energy from these sources should be considered when doing a complete energy balance for the snowpack.

Errors in the measurements of temperature and also from uncertainties in the spacing between thermistors affect the calculation of the divergence of the temperature gradient. The resolution of the temperature measurements was better than ±0.01°C, and changing the temperature of $T_{x,z}$ by +0.01°C in the calculations shown in Figure 3b changed the flux divergence before infiltration by less than 3%. This effect is small compared with other uncertainties. Uncertainties in the spacing between thermistors had a much larger effect. Although the resolution of settlement measurements was better than ±0.2 mm, we suspect that the error in the spacing between thermistors could be as much as 1–2 cm. Part of the error is caused by differential snow settlement which often displaced thermistors on the same horizontal string by varying distances. Decreasing the vertical spacing between $T_{x,z}$ and the surrounding thermistors (while keeping all other parameters constant) by 1 cm (about 10%) increased the flux divergence before infiltration by about 25%. If the spacing was decreased by 20% or 2 cm, the flux divergence increased by 60%. Although the uncertainties have a major impact on the calculation for dry snow, they are less significant during infiltration because at first the release of latent heat dominates the process and later, when the snowpack is isothermal, the net heat transfer is zero, and the spacing between thermistors is not relevant to the calculation.

Measurements of snow temperature define the thermal conditions in snowpacks and can help define the characteristics of infiltration in subfreezing snow. The measurements show clearly the evolution in time and space of the three distinct zones (dry, transition, and wet zones) during wetting of snowpacks. Arrays of heat transducers or dielectric devices could also be used, but thermistors are relatively inexpensive, nonintrusive, and easy to use compared with these other devices. Measurements of temperature would be less useful for tracking infiltration in isothermal snowpacks that were already near 0°C. Further, the technique would have limited use for determining the arrival time of water at the base of many maritime snowpacks because in our experience the temperature at that interface is usually near 0°C.

The observation that on a few occasions a thermistor warmed to 0°C more slowly than the surrounding thermistors is evidence that infiltration is three dimensional. It would be best to have a three-dimensional array of thermistors, but there are a number of practical difficulties associated with the installation of such an array. An alternative method to improve the spatial resolution of the infiltration process would be to use a two-dimensional array of thermistors that was wider and more closely spaced than that used in our study.

Rates and Patterns of Wetting

The patterns and rate of infiltration depend on the flux of liquid water as well as the hydraulic properties of the snowpack. The liquid water flux depends not only on the rate of precipitation but also on the rate of freezing as determined by the thermal conditions in the snowpack. In the two examples discussed here the total amount of freezing required to warm the snow to near 0°C was small compared with the total influx of rainwater. We suspect that this behavior is typical for maritime snowpacks. In other climates where snow temperatures are colder and midwinter rainfall is less, it is possible that the thermal requirements of the snowpack would have a larger impact on the infiltration process.

The hydraulic conductivity of porous media depends on both the permeability and capillarity, and these properties vary widely depending on grain size and texture [*Wankiewicz*, 1979; *Colbeck*, 1979]. Changes in stratigraphy further complicate infiltration because pressure differences often develop across textural boundaries, and flow is diverted laterally until the pressure difference across the boundary is relieved in some way [*Glass et al.*, 1989a, b]. In snow the problem of characterizing infiltration is further complicated because the presence of liquid water may cause significant textural changes over time scales that are shorter than those for infiltration.

We characterize the pattern of wetting by considering the

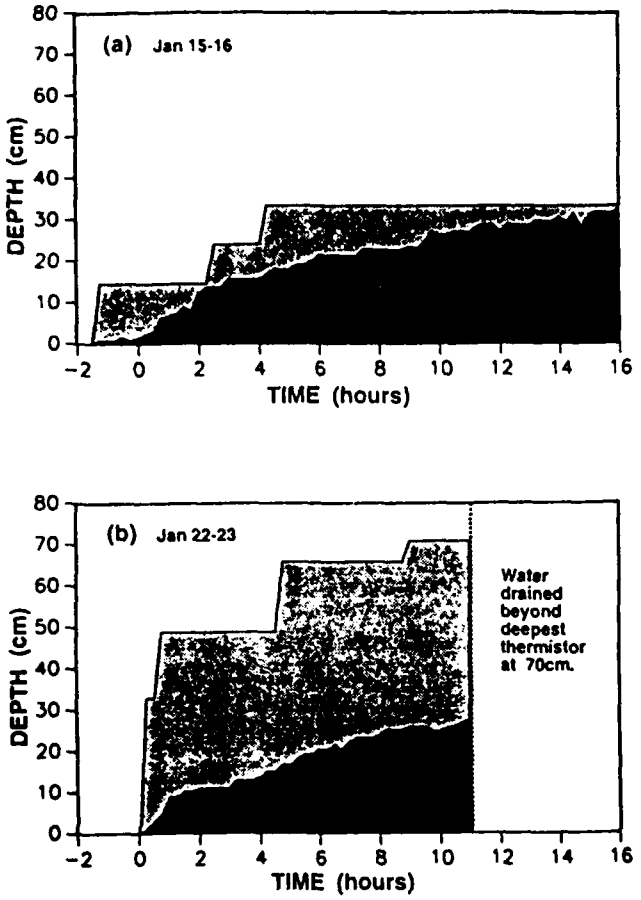

Figure 6. Evolution of the pattern and depth of wetting. The maximum depth of water penetration is shaded gray and the "equivalent wetted thickness" or depth of background wetting is shaded black. The difference between these depths is a measure of the uniformity of wetting. (a) Depth of wetting on January 15–16. Meltwater had penetrated 15 cm before rain started. Infiltration progressed in a "step and fill" pattern. The depth of each step was controlled by the spacing between stratigraphic horizons. (b) Depth of wetting on January 22–23. Liquid water penetrated 50 cm into the snowpack during the first 45 min of rain through localized channels. Less than 50% of the snowpack had been wetted when water drained beyond the deepest thermistor 11 hours after rain started.

maximum depth of water penetration and the "equivalent wetted thickness" of snow. The equivalent wetted thickness is the total volume of wetted snow per unit area and could be thought of as the depth of background wetting. The difference between the depths of the wetting front and the background wetting is a measure of the uniformity of wetting. Figure 6 shows a time series of each of these characteristics at 15-min intervals. On January 22 the depth of background wetting typically lagged the wetting front by 50% or more (see Figure 6b), indicating that less than half of the volume of snow above the wetting front had been wetted. In contrast, on January 15 the background wetting and the wetting front were much closer together (see Figure 6a), and wetting was more uniform.

The plots show the "step and fill" pattern of wetting mentioned earlier. The finite spacing between thermistors and the discrete time between measurements would contribute to step-type behavior, but we expect that the depth of each step is more closely related to the vertical spacing between textural horizons, and the time between steps depends on the time taken to relieve the pressure mismatch across each horizon.

Figure 6 also shows that water penetrated to depth much faster on January 22–23 than on January 15–16. The overall rate of wetting was similar for each event (as shown by a comparison of changes in the equivalent wetted thickness for each event), which suggests that the different behavior was caused primarily by differences in the hydraulic conductivity. The texture and stratigraphy of the snowpack was altered significantly during the rain on January 15 and 16. Grains had coarsened in zones that had been wet, and the larger grain size would increase the hydraulic conductivity [*Glass et al.*, 1989a]. Further, differential snow settlement during the first event caused the surface to be undulating. It is probable that the undulations were preserved beneath the new snow that had accumulated before the 22, and subsequent water arriving at that horizon would tend to be concentrated into the depressions. These effects could also contribute to increase the rate of vertical infiltration during the second event. This type of behavior has also been reported by *McGurk and Kattelmann* [1986], who observed increased rates of drainage as a snowpack became more homogeneous.

In both cases, vertical flow was impeded for several hours at ice crusts. Although this is not surprising given the low permeability of ice, it is different from our earlier observations that water usually penetrates ice layers rapidly in maritime snowpacks [*Conway and Raymond*, 1993]. The earlier observations were based on dye tracing experiments, and it is possible that in those cases the hydraulic properties were affected by the snow pits that were needed to make the observations. Alternatively, we expect large variations in the permeability of ice crusts which could also contribute to the different behavior.

Timing of Outflow

Predicting the timing of outflow from snowpacks is of interest for hydrological modeling. Here we use our results to obtain an order of magnitude estimate of the time of outflow from a maritime snowpack. Results indicate that although freezing has a major impact on the heat equation, the amount of water needed to change phase in order to satisfy the heat equation in maritime snowpacks is small. If we neglect losses due to freezing, after t hours a total of ($t \times PI$) millimeters of water would have entered the snowpack (PI is the average rain intensity in millimeters per hour).

Results also indicate that water often penetrates through channels that occupy about 50% of the snowpack, and the moisture content of wet snow during infiltration is about 10% by volume. If these general findings are combined, the time taken for water to penetrate to a depth Z in a snowpack is

$$t = \frac{0.1(0.5Z)}{PI\ 10^{-3}} = 50\,\frac{Z}{PI} \tag{6}$$

Maritime snowpacks are often 1.5 to 3 m deep, and although the rate of rainfall varies widely, rates typically

range from 2 to 5 mm h^{-1}. Using these assumptions, we expect drainage would commence 15 to 75 hours after the onset of rain.

Conclusions

Measurements from a spatial array of thermistors can be used to track the progress of liquid water into subfreezing snowpacks. Warming and infiltration into snow is not homogeneous, and a single line of thermistors arranged vertically in a snowpack is not adequate to define the thermal conditions. It would be best to use a three-dimensional array of thermistors, but this would be difficult to install and would increase disturbances of the snowpack. Two-dimensional arrays are easier to manage and yet still yield information about infiltration processes. The array used in this study could be improved by extending the width by at least 1 m and also by installing thermistors through the full depth of the snowpack.

The latent heat released when liquid water freezes on contact with cold snow dominates heat transfer processes at the wetting front. The amount of freezing needed to warm maritime snowpacks to near 0°C is small compared to the amount of rain that typically falls during midwinter events in maritime climates. Most of the influx of rainwater remains in the liquid phase. This may not be true in climates where snow temperatures are colder and the total rainfall during storms is less. In these cases, larger fractions of the rainwater may need to freeze in order to satisfy the heat equation, and this may have a significant impact on the infiltration process.

Thermal conditions play a relatively minor role in maritime snowpacks, and most of the influx of rainwater is available to wet and then drain through the snowpack. Infiltration is controlled primarily by the hydraulic conditions. Stratigraphic horizons that exist in natural snowpacks make it difficult to characterize simply the hydraulic conductivity. The problem is compounded because conductivity may change significantly as a result of grain-coarsening processes associated with wetting. Further studies are needed to characterize the hydraulic conductivity across various textural boundaries and horizons. Other things being equal, water will penetrate a homogeneous, coarse-grained snowpack faster than a snowpack that contains multiple stratigraphic horizons.

Acknowledgments. This research was funded by the U.S. Army Research Office (grant DAAL03-91-G-0143). We also wish to thank Charlie Raymond, Matthew Sturm, Craig Wilbour, Steve Breyfogle, Lee Reddon, and Joe Wilson, who assisted with the research.

References

Colbeck, S. C., Water flow through heterogeneous snow, *Cold Reg. Sci. Technol.*, *1*(1), 37–45, 1979.

Colbeck, S. C., et al., The international classification for snow on the ground, report, 23 pp., Int. Comm. on Snow and Ice, Int. Assoc. of Hydrol. Sci., Gentbrugge, Belgium, 1990.

Conway, H., and R. Benedict, Measurements of snow temperature during rain, paper presented at International Snow Science Workshop, Breckenridge, Co, 1992.

Conway, H., and C. F. Raymond, Snow stability during rain, *J. Glaciol.*, in press, 1993.

Gerdel, R. W., The transmission of water through snow, *Eos Trans. AGU*, *35*, 475–485, 1954.

Glass, R. J., T. S. Steenhuis, and J-Y. Parlange, Wetting front instability, 1, Theoretical discussion and dimensional analysis, *Water Resour. Res.*, *25*(6), 1187–1194, 1989a.

Glass, R. J., T. S. Steenhuis, and J-Y. Parlange, Wetting front instability, 2, Experimental determination of relationships between system parameters and two-dimensional unstable flow field behavior in initially dry porous media, *Water Resour. Res.*, *25*(6), 1195–1207, 1989b.

Kattelmann, R. C., Macropores in snowpacks of Sierra Nevada, *Ann. Glaciol.*, *6*, 272–273, 1985.

Kattelmann, R. C., Spatial variability of snow-pack outflow at a site in Sierra Nevada, USA, *Ann. Glaciol.*, *13*, 124–128, 1989.

Marsh, P., and M. K. Woo, Wetting front advance and freezing of meltwater within a snowcover, 1, Observations in the Canadian Arctic, *Water Resour. Res.*, *20*, 1853–1864, 1984.

Marsh, P., and M. K. Woo, Meltwater movement in natural heterogeneous snow covers, *Water Resour. Res.*, *21*, 1710–1716, 1985.

McGurk, B. J., and R. C. Kattelmann, Water flow rates, porosity, and permeability in snowpacks in the central Sierra Nevada, in *Cold Regions Hydrology Symposium*, edited by D. L. Kane, pp. 359–366, American Water Resources Association, Minneapolis, Minn, 1986.

Pfeffer, W. T., T. H. Illangasekare, and M. F. Meier, Analysis and modeling of melt-water refreezing in dry snow, *J. Glaciol.*, *36*(123), 238–246, 1990.

Press, W. H., B. P. Flannery, S. A. Teukolsky, and W. T. Vetterling, *Numerical Recipes; The Art of Scientific Computing*, Cambridge University Press, New York, 1986.

Raymond, C. F., and K. Tusima, Grain coarsening of water-saturated snow, *J. Glaciol.*, 22(86), 83–105, 1979.

Sturm, M., and J. Holmgren, Rain-induced water percolation in snow detected using heat flux transducers, *Water Resour. Res.*, *29*(7), 2323–2334, 1993.

Wakahama, G., The role of meltwater in densification processes of snow and firn, *IASH Publ.*, *114*, 66–72, 1975.

Wankiewicz, A. C., A review of water movement in snow, in Proceedings of the Modeling of Snow Cover Runoff, edited by S. C. Colbeck and M. Ray, *CRREL Spec. Rep. 79-36*, pp. 222–252, Cold Reg. Res. and Eng. Lab., Hanover, N. H., 1979.

Yen, Y.-C., Review of thermal properties of snow, ice and sea ice, *CRREL Rep. 81-10*, 27 pp., Cold Reg. Res. and Eng. Lab., Hanover, N. H., 1981.

R. Benedict and H. Conway, Graduate Program in Geophysics, AK-50, University of Washington, Seattle, WA 98195.

(Received March 1, 1993; revised November 4, 1993; accepted November 15, 1993.)